Scalable node-disjoint and edge-disjoint multiwavelength routing

Yi-Zhi Xu [1], Ho Fai Po [2], Chi Ho Yeung [2], and David Saad [1,*]

[1]*The Nonlinearity and Complexity Research Group, Aston University, Birmingham B4 7ET, United Kingdom*

[2]*Department of Science and Environmental Studies, The Education University of Hong Kong, 10 Lo Ping Road, Taipo, Hong Kong*

(Received 29 June 2021; revised 7 July 2021; accepted 7 April 2022; published 21 April 2022)

Probabilistic message-passing algorithms are developed for routing transmissions in multiwavelength optical communication networks, under node- and edge-disjoint routing constraints and for various objective functions. Global routing optimization is a hard computational task on its own but is made much more difficult under the node- and edge-disjoint constraints and in the presence of multiple wavelengths, a problem which dominates routing efficiency in real optical communication networks that carry most of the world's internet traffic. The scalable principled method we have developed is exact on trees but provides good approximate solutions on locally treelike graphs. It accommodates a variety of objective functions that correspond to low latency, load balancing, and consolidation of routes and can be easily extended to include heterogeneous signal-to-noise values on edges and a restriction on the available wavelengths per edge. It can be used for routing and managing transmissions on existing topologies as well as for designing and modifying optical communication networks. Additionally, it provides the tool for settling an open and much-debated question on the merit of wavelength-switching nodes and the added capabilities they provide. The methods have been tested on generated networks such as random-regular, Erdős Rényi, and power-law graphs, as well as on optical communication networks in the United Kingdom and United States. They show excellent performance with respect to existing methodology on small networks and have been scaled up to network sizes that are beyond the reach of most existing algorithms.

DOI: 10.1103/PhysRevE.105.044316

I. INTRODUCTION

Optical communication networks underpin the global digital communications infrastructure and carry most of the internet traffic. They comprise thousands of kilometers of optical fibers, organized in a complex web of constituent subnetworks including the internet backbone, Metro access and Data Center farms. The exponential growth in internet traffic and energy consumption threatens to overload the existing infrastructure and a capacity crunch is looming [1]. Not only that a matching growth in infrastructure is infeasible, it raises fundamental questions on the ultimate capacity of optical communication networks and the manner in which we could optimize their use. The next-generation digital infrastructure has to offer flexibility, low latency, high network throughput, and resilience.

One of the key requirements is the routing and wavelength assignment (RWA) for all traffic demands across this complex heterogeneous network in a way that optimizes a given objective function, be it low latency, high throughput, or resilience [2–4]. Each optical fiber carries information using light of one or many wavelengths. The latter uses, among others, dense wavelength-division multiplexing (DWDM) methods that employ as many as 80–160 channels of different laser wavelengths [5]. The main constraint in the RWA is that any complete individual route, from source to destination, uses the same single wavelength and that two separate routes using the same wavelength cannot shares the same fiber. This constraint makes the corresponding mathematical problem hard to solve in general.

Route optimization in optical communication networks can be mapped onto the hard computational problem of edge-disjoint routing on a graph, where transceivers (transmitter-receiver) are mapped to vertices (or nodes) and fibers to edges (or links). Given that routes are constrained to be contiguous and interaction between paths is nonlocalized, local optimization methods are insufficient and global optimization is required. Globally optimal routing of multiple messages or vehicles given a general objective function is a computationally hard constraint satisfaction problems on its own and has been addressed in the physics literature using scalable and distributed message passing approximation techniques, inspired by statistical physics methodology [6–9]. Moreover, similar techniques have been suggested also for addressing the *single-wavelength* node-disjoint paths (NDP) [10] and edge-disjoint paths (EDP) [11] problems where multiple paths of different origin-destination pairs cannot share nodes or edges on a graph, respectively. Generally, both optimization tasks are within the class of NP-hard combinatorial problems [12–15] and the approximation offered by message passing techniques work well. However, the existing methods developed for single-wavelength routing become intractable in the presence of multiple wavelengths, making them inapplicable for realistic scenarios.

It is worthwhile noting that in some extreme cases these hard computational problems become polynomial in the single wavelength case as discussed in Ref. [11]. For instance, when the number of origin-destination pairs is low with respect to the systems size [16] and where all origin-destination pairs are identical [17,18]. Nevertheless, the general problems

*Corresponding author: d.saad@aston.ac.uk

of NDP and EDP routing on graphs are computationally hard even in the single wavelength case and a variety of methods have been used to address them in the context of optical communication networks and more general problems. Alongside established methods, such as integer and linear programming and its variants [19–23] bin-packing-based approaches [24], Monte Carlo search [25], post-optimization [26], and greedy algorithms [27–30], a large number of heuristics have also been used to obtain approximate solutions in both problems, among them genetic algorithms [31–33], ant colony optimization [34], and particle swarm optimization [35]. Specifically in the area of optical communication networks, it is common to use integer and linear programming and its variants for small networks, to obtain exact results, and a variety of heuristics for larger networks. In practice, current optical networks use overprovision of capacity to compensate for suboptimal routing, resulting in both overengineering and underutilized capacity [36,37].

The main challenge we address here is the RWA under heavy traffic using *multiple wavelengths* and a very large number of origin-destination pairs under the NDP and EDP constraints and for various objective functions. Globally optimal routing is a nonlocalized difficult problem but adding the NDP/EDP restrictions and having a large number of different wavelengths increases the complexity considerably, making the problem intractable (exponential) for existing algorithms [10,11]. We map the globally optimal routing problem in the presence of multiple wavelengths onto a multilayer replica of the original graph and utilize probabilistic optimization approaches. The methods developed here are based on message passing techniques, developed independently in several fields including statistical physics, computer science and information theory [38–40] but are closely interlinked [41,42]. The methods we develop allow for messages, in the form of conditional probability values to be passed between *nodes and the replicated networks representing the different wavelengths*, in a way that keeps the algorithms scalable and applicable even for a large number of wavelengths, transmissions (corresponding to source-destination pairs) and nodes.

The main result of this paper is the derivation of principled scalable algorithms, capable of obtaining approximate solutions for routing problems in large graphs, where the number of transmissions is of similar order to that of the number of free variables (vertices/edges) and a large number of wavelengths, under the NDP and EDP constraints and for various objective functions, both convex and concave. The algorithm also accommodate cases where the number of transmissions is much larger than the number of vertices (quadratic with respect to the number of vertices). The computational complexity of the NDP/EDP algorithms for sparse graphs is $O[MQ(M+N+Q)]/O[MQ(M/N+N+Q)]$, with N the number of vertices, M the number of transmissions, and Q the number of wavelengths. The algorithm has been tested for a variety of sparse network topologies, both synthetic random graphs and real optical communication networks, and for different objective functions, showing excellent results in obtaining high quality approximate solutions. Among the generic networks examined are random regular graphs, Erdős Rényi (ER) [43] and scale-free networks [44], while the realistic networks considered include the British 22 nodes (BT22) [45] and U.S. 60 node (CONUS) [46] backbone optical communication networks. When tested on small networks against known results obtainable using unscalable methods like variants of integer and linear programming, it was shown to provide the optimal routing results.

The results provide the maximal number of communication pairs that could be accommodated given the network size, topology, and number of wavelengths used; the minimal number of wavelengths required for a given network, topology, and communication pairs; and the resulting utilization of edges. They identify the impact of using the suggested algorithm on the average path length, the utilization of wavelengths per edge and how it can be controlled using concave and convex objective functions.

In addition, our algorithms can be used for routing transmissions across networks in single instances, study the limitations of heterogeneous networks of different degree distributions, with variable edge signal-to-noise ratios and wavelength availability. Moreover, our algorithms could be employed in the design of new infrastructure, especially through the use of concave cost functions that consolidate routes, by determining the least important routes that could be removed with little effect on the network throughput or resilience. These are of both academic and practical values since the performance of optical communication networks is often directly related to their capacity limits, traffic congestion, rate of information flow and bandwidth flexibility. Moreover, we also studied a switching model, where wavelength can be converted (switched) at the vertices (transceivers) to settle an open and much debated question on the merit of wavelength-converters [47–49] for increasing throughput, resource utilization and resilience in optical communication networks.

While we mainly focus here on the optical communication network application and test the efficacy of the method on networks and number of wavelengths that are relevant to this application domain, one should point out that these problems are highly relevant to other domains. For instance, multiwavelength NDP/EDP are relevant to both 5G and the future 6G wireless communication systems and wireless ad-hoc communication networks in the relay setting, where each node can act as a relay. Our algorithms can reduce path overlaps, which represent transmissions in similar wavelength, resulting in signal interference and low transmission quality, or to consolidate paths since longer paths result in signal degradation and the need for higher transmission power [28,29,50]. Another application is the design of very large system multilayer integrated circuits (VLSI), where nonoverlapping wired paths to connect different components are sought to avoid cross-path interference. In all cases, higher throughput, robustness, and lower latency can be achieved for the same resource by obtaining a good approximation to the globally optimal solution. Practical algorithms for various applications often depend on the specific network topologies considered [51] and are aimed at maximizing the number of paths routed [52].

The reminder of the paper is organized as follows: In Sec. II we introduce the model used followed by the message-passing based algorithmic solutions for NDP, EDP, and wavelength switching scenarios in Sec. III. Results obtained from numerical studies on a range of synthetic and real networks and a variety of objective functions are presented in Sec. IV

followed by a discussion on their computational complexity. Possible extensions of the framework to accommodate real-world scenarios such as edges with different signal-to-noise ratios or wavelength availability are presented in Sec. V. Finally, we discuss the efficacy of the methods developed and point to future research directions in Sec. VI.

II. MODEL

We consider a dense wavelength-division multiplexing (DWDM) optical network $G(V, E)$, with $V \equiv \{i \mid i \in G\}$ and $|V| = N$, the set of nodes representing transceivers and $E \equiv \{(i, j) \mid (i, j) \in G\}$ the set of edges, such that the indices (i, j) represent the optical fiber between node i and j. For a network which uses Q wavelength channels to deliver M transmissions, we introduce a Q-dimensional vector $\vec{s}_{i,j}$ on the link from node i to j such that its ath entry $s^a_{i,j} = s$ or $-s$ if transmission s passes from node i to j or from j to i, respectively, through link (i, j) using wavelength a; the transmission s corresponds to one of the origin-destination pair $\{1, \ldots, M\}$, and $s^a_{i,j} = 0$ denotes that no communication uses wavelength a on link (i, j). A similar Q-dimensional vector $\vec{s}_i$ is defined for node i in the case of NDP, where the component s^a_i takes the value $\{0, 1, \ldots, M\}$, representing the use of wavelength a on node i by request s if $s^a_i = s \neq 0$, or $s^a_i = 0$ if it is not occupied by any transmission. Since each transmission has to occupy an individual wavelength channel on a link, more wavelengths are generally required for more transmissions, i.e., a larger value of Q is required for a larger M. For specific network instances with Q wavelength channels, there exists a maximum number of transmissions denoted as $M_{\max}$ which can be transmitted; alternatively, one can define the minimum number of wavelength channels, i.e., $Q_{\min}$, which accommodate all M transmissions on a specific instance. The relationship between $M_{\max}$ and Q, or between M and $Q_{\min}$, would be highly relevant for characterizing the maximum capacity of optical networks.

This framework can accommodate a variety of objective functions; here, we consider the sum of the cost (or utility) on each link to be the objective function for optimization, given by

$$H(\vec{\vec{s}}) = \sum_{(i,j)} F_{i,j}\left(Q - \sum_{a=1}^{Q} \delta^0_{s^a_{i,j}}\right), \tag{1}$$

where δ^y_x is the Kronecker δ such that $\delta^y_x = 1$ if $x = y$ and $\delta^y_x = 0$ otherwise; the function $F_{i,j}$ denotes the cost on link (i, j) as a function of the argument in parenthesis; while it can take an arbitrary form we will mostly focus on simple polynomial functions. In the context of statistical physics, we introduce the inverse temperature β, and the partition function Z of the system is given by

$$Z(\beta) = \sum_{\vec{\vec{s}}} \Omega(\vec{\vec{s}}) e^{-\beta H(\vec{\vec{s}})} = \sum_{\vec{\vec{s}}} \Omega(\vec{\vec{s}}) \prod_{(i,j)} e^{-\beta F_{i,j}(\vec{s}_{i,j})}, \tag{2}$$

where $\vec{\vec{s}} \equiv \{\vec{s}_{i,j}\} \otimes \{\vec{s}_i\}$ denotes the configurations of communication routes through all links and nodes on the network, and $\Omega(\vec{\vec{s}})$ is an indicator function such that $\Omega(\vec{\vec{s}}) = 1$ if $\vec{\vec{s}}$ satisfies all the constraints of the problem or otherwise $\Omega(\vec{\vec{s}}) = 0$. The double vector notation comes to emphasize dependence on both topology and wavelength.

We now summarize the constraints of the optimization problem. First, the route for each transmission must be contiguous. A loopless path is a sequence of nonrepeating nodes from origin to destination, for example, path s is constructed as $O_s \to \cdots \to j \to i \to k \to \cdots \to D_s$, where O_s and D_s are the origin and destination pair of transmission s. Second, for an intermediate node i along the path there exist only two used edges (j, i) and (i, k) for that wavelength and transmission. This constraint could be expressed as follows: If $s^a_{i,j} = s \neq 0$, then

$$\sum_{k \in \partial i \setminus j} \left(1 - \delta^0_{s^a_{i,k}}\right) = 1 \text{ and } \sum_{k \in \partial i \setminus j} s^a_{i,k} = -s, \tag{3}$$

where $\partial i \equiv \{j \mid (i, j) \in E\}$ is the set of the nearest neighbors of node i, and $\partial i \setminus j \equiv \partial i - \{j\}$ is the subset of ∂i except node j. Regarding the wavelength constraints along the path, we will consider three scenarios in the subsequent analyses:

(1) *Node-disjoint paths* (NDP)—where only a single transmission is allowed to utilize a specific wavelength channel on a node [10], but there can be multiple transmissions using different channels through the same node as shown in Fig. 1(a); this may correspond to transceivers which can only process a single transmission for each individual wavelength. The expression of the node-disjoint constraint is $s^a_{i,j} = s \neq 0 \Rightarrow \forall k \in \partial i \setminus j : s^a_{i,k} \in \{0, -s\}$.

(2) *Wavelength-switching* (WS) with NDP—where all incoming or outgoing transmissions to transceivers (nodes) use different wavelength channels, but transmissions are allowed to switch between wavelength channels at the transceivers as shown in Fig. 1(b), leading to a larger routing flexibility.

(3) *Edge-disjoint paths* (EDP)—where multiple transmissions using the same wavelength channel, are allowed to be routed through any given node [11] but cannot share an edge, as shown in Fig. 1(c). This is the typical scenario in optical communication networks.

III. MESSAGE-PASSING ALGORITHMS

To derive optimization algorithms to allocate simultaneously the optimal route and wavelength for a large number of transmissions, we solve the problem on multilayer graphs where each layer represents a different wavelength, and messages are passed within each layer for assignment of routes and between layers for allocation of wavelength. By applying the cavity approach from the study of spin glass systems [38,41,53], we can derive distributed message-passing algorithms for optimizing transmission routes in optical networks for NDP, WS and EDP scenarios.

It should be noted that there is interaction between layers at each edge/vertex through the objective function that depends on the local wavelength allocation per communication request. This is manifested through the dynamically passed messages prior to the inference decisions made with respect to wavelength and route allocation. Additionally, the factor graphs that correspond to the different routing scenarios are loopy and the derived algorithms exploit the differences in strength between the different interaction types, within and across layers. A more detailed explanation of the respective

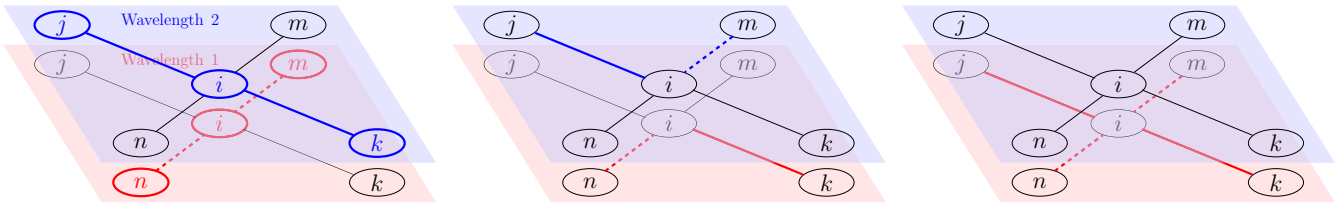

(a) Node-disjoint (b) Node-disjoint wavelength-switching (c) Edge-disjoint

FIG. 1. An exemplar graph with $N = 5$ nodes and 4 edges, where $M = 2$ transmissions with origins and destinations j and k (solid), and m and n (dashed), respectively, are transmitted by $Q = 2$ wavelength channels represented by the red and blue layers. (a) The node-disjoint (NDP) case, where the whole transmission path uses the same wavelength. For instance, the red wavelength channel of node i is used by the transmission from $m \to n$, so the red node i cannot be a part of the other transmission from $j \to k$, which instead uses the blue wavelength channel. (b) The wavelength-switching scenario of NDP (WS), where the two transmission switch their wavelength channels at node i; panels (a) and (b) are valid under this switching scenario. (c) The edge-disjoint (EDP) case, where the red layer is sufficient for accommodating the two transmissions, and the blue layer is idle.

factor graphs and the assumptions made is provided in the Appendix.

A. Node-disjoint routing

First, we consider the NDP routing scenario [10] shown in Fig. 1(a). The network is represented by a factor graph with two types of variables, namely s_i^a defined on nodes and $s_{i,j}^a$ defined on links. According to the Bethe-Peierls approximation [54,55], we assume only large loops exist in the network such that all neighboring nodes and edges of a node i are nearly independent in the absence of i.

To derive the *multiwavelength routing* algorithm, we first define $p_{i\to j}$ to be the message from node i to edge (i, j) and $q_{i\to j}$ to be the message from edge (i, j) to node j. Both messages are conditional probabilities: $p_{i\to j}(s)$ is the probability of edge (i, j) to be in state s due to the state of node i and $q_{i\to j}(s)$ the probability of edge (i, j) to be in state s without the interaction from node i. We then write a closed set of recursion relations to express the message $p_{i\to j}$ in terms of $q_{k\to i}$, as well as another set of relations representing $q_{i\to j}$ in terms of $p_{i\to j}$ and $p_{j\to i}$:

$$
\begin{aligned}
p^a_{i\to j}(0) &\propto \prod_{k\in\partial i\setminus j} q^a_{k\to i}(0) \\
&\quad + \sum_{\substack{m,n\in\partial i\setminus j \\ s\neq 0}} q^a_{m\to i}(s) q^a_{n\to i}(-s) \prod_{k\in\partial i\setminus j,m,n} q^a_{k\to i}(0), \\
p^a_{i\to j}(s) &\propto \sum_{k\in\partial i\setminus j} q^a_{k\to i}(s) \prod_{l\in\partial i\setminus j,k} q^a_{l\to i}(0); \\
q^a_{i\to j}(0) &\propto p^a_{i\to j}(0) \sum_n e^{-\beta F_{i,j}(n)} \sum_{\substack{b\neq a: \\ s^b=0,1}} \delta^n_{\sum_{b\neq a} s^b} \prod_{b\neq a} \tilde{q}^b_{i,j}(s^b), \\
q^a_{i\to j}(s) &\propto p^a_{i\to j}(s) \sum_n e^{-\beta F_{i,j}(n+1)} \sum_{\substack{b\neq a: \\ s^b=0,1}} \delta^n_{\sum_{b\neq a} s^b} \prod_{b\neq a} \tilde{q}^b_{i,j}(s^b),
\end{aligned}
\tag{4}
$$

where we have further defined the auxiliary quantities $\tilde{q}^b_{i,j}$ given by

$$
\begin{aligned}
\tilde{q}^a_{i,j}(0) = \hat{q}^a_{i,j}(0), \quad \tilde{q}^a_{i,j}(1) = \sum_{s\neq 0} \hat{q}^a_{i,j}(s); \\
\hat{q}^a_{i,j}(s) = p^a_{i\to j}(s)\, p^a_{j\to i}(-s).
\end{aligned}
\tag{5}
$$

For brevity we omit the normalization term and use the notation "$\propto$" instead of the equality symbol. For a brief explanation of how these equations are construed: The first equation of Eq. (4), looks at the probability for no transmission on the edge $i \to j$, as a summation of the probability of no transmission entering i (first term) and the probability of transmissions arriving at i from node m but leaving

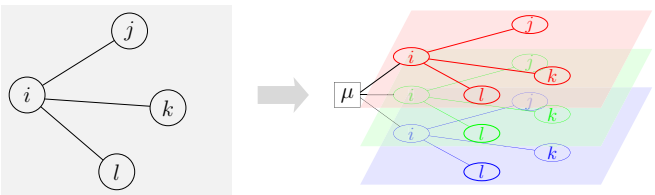

(a)

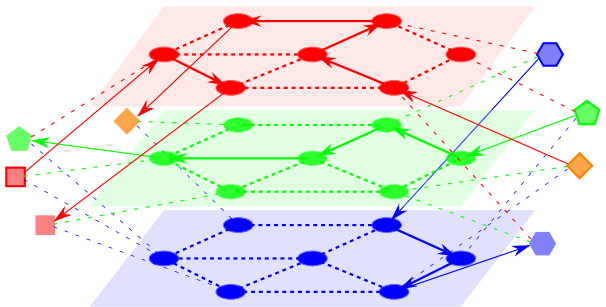

(b)

FIG. 2. (a) Mapping the original network (left) onto multilayer replica networks that use different wavelengths (right). In this example, node i is the origin/destination of transmission $|\mu|$. Introducing an auxiliary node μ, denoted by a square and connected to nodes i at each of the layers, facilitates message passing between the new node and the different layers to determine the allocation of transmissions to wavelengths. These auxiliary nodes also facilitate the interaction among different wavelengths. (b) An example of routing paths on a simple network with $N = 7$ nodes and $M = 4$ transmissions, which shows the complete algorithmic framework with wavelengths as colored layers, origins and destinations as auxiliary nodes denoted by framed and un-framed noncircular symbols, respectively, transmission paths as colored solid lines with arrows and un-occupied wavelength channels as colored dotted lines.

through some other node n (second term); the second equation looks at the message s arriving at node i but not leaving through any other edge but $i \to j$; the third and fourth equations describe the probability of edge $i \to j$ to be in a given state 0 or s, given the related cost on the edge, in conjunction with all other wavelengths. In Eq. (4), node messages using wavelength a depend only on the messages from their neighbors using the same wavelength and the network is effectively mapped onto a system with Q separate layers, each of which employs a different wavelength channel, as shown in Fig. 1(a); the interdependence between wavelengths is considered at the origin and destination of individual transmissions [Fig. 2(a)], as discussed below. An example of the complete routing is described in Fig. 2(b).

With the messages $p_{i\to j}$ and $q_{i\to j}$ having converged to stable values, one can express the marginal probability of node i being in state s using wavelength a as

$$p_i^a(0) \propto \prod_{j\in\partial i} q_{j\to i}^a(0), \quad p_i^a(s) \propto \sum_{m,n\in\partial i} q_{m\to i}^a(s) q_{n\to i}^a(-s) \prod_{j\in\partial i\backslash m,n} q_{j\to i}^a(0). \tag{6}$$

The marginal probability of edge (i, j) being in state s with wavelength a is given by

$$q_{i,j}^a(0) \propto \hat{q}_{i,j}^a(0) \cdot \sum_n e^{-\beta F_{i,j}(n)} \sum_{\substack{b\neq a:\\ s^b=0,1}} \delta^n_{\sum_{b\neq a} s^b} \prod_{b\neq a} \tilde{q}_{i,j}^b(s^b), \quad q_{i,j}^a(s) \propto \hat{q}_{i,j}^a(s) \cdot \sum_n e^{-\beta F_{i,j}(n+1)} \sum_{\substack{b\neq a:\\ s^b=0,1}} \delta^n_{\sum_{b\neq a} s^b} \prod_{b\neq a} \tilde{q}_{i,j}^b(s^b), \tag{7}$$

where the factors after the dot symbols correspond to contributions from all neighboring links of (i, j) to the partition function, which takes into account all possible variable configurations in the trees terminated at the neighboring edges.

To simplify the algorithms, we introduce the variables $\phi \equiv -\frac{1}{\beta}\log q$ and $\psi \equiv -\frac{1}{\beta}\log p$, and take the zero-temperature limit for optimization $\beta \to \infty$. The components of ϕ and ψ are real numbers, and can take any value in $\mathbb{R}$. The recursion relations of messages in Eq. (4) thus become equivalent to the min-sum belief propagation relations [41], given by

$$\begin{aligned}
&\psi_{i\to j}^a(0) = \min\left\{ \sum_{k\in\partial i\backslash j} \phi_{k\to i}^a(0), \min_{\substack{m,n\in\partial i\backslash j\\ s\neq 0}} \left[\phi_{m\to i}^a(s) + \phi_{n\to i}^a(-s) + \sum_{k\in\partial i\backslash j,m,n} \phi_{k\to i}^a(0) \right] \right\},\\
&\psi_{i\to j}^a(s) = \min_{k\in\partial i\backslash j} \left[\phi_{k\to i}^a(s) + \sum_{l\in\partial i\backslash j,k} \phi_{l\to i}^a(0) \right]; \quad \phi_{i\to j}^a(0) = \psi_{i\to j}^a(0) + \min_n \left[F_{i,j}(n) + \min_{\substack{\sum_{b\neq a} s^b = n:\\ s^b=0,1}} \sum_{b\neq a} \tilde{\phi}_{i,j}^b(s^b) \right],\\
&\phi_{i\to j}^a(s) = \psi_{i\to j}^a(s) + \min_n \left[F_{i,j}(n+1) + \min_{\substack{\sum_{b\neq a} s^b = n:\\ s^b=0,1}} \sum_{b\neq a} \tilde{\phi}_{i,j}^b(s^b) \right],
\end{aligned} \tag{8}$$

where

$$\tilde{\phi}_{i,j}^a(0) = \psi_{i\to j}^a(0) + \psi_{j\to i}^a(0), \quad \tilde{\phi}_{i,j}^a(1) = \min_{s\neq 0}[\psi_{i\to j}^a(s) + \psi_{j\to i}^a(-s)]. \tag{9}$$

For each individual transmission $|\mu| \in \{1, \ldots, M\}$, we then introduce auxiliary nodes labeled as $\mu = \pm|\mu| \in \{\pm 1, \cdots, \pm M\}$, where nodes with positive and negative μ connect to origin and destination nodes, respectively, in each of the Q wavelength network layers, respectively [see in Fig. 2(a)]. These auxiliary origin-destination pairs of each transmission communicate with all wavelength replica networks to determine the path and wavelength channel allocated to each transmission, using the message passing algorithm, given by

$$\phi_{\mu\to a}(0) = \min_{b\neq a} \left[\phi_{b\to\mu}(-\mu) + \sum_{c\neq a,b} \phi_{c\to\mu}(0) \right], \quad \phi_{\mu\to a}(\mu) = 1 + \sum_{b\neq a} \phi_{b\to\mu}(0), \quad \phi_{\mu\to a}(s) = \infty, \quad s \neq 0, \mu, \tag{10}$$

such that the transmission routes are determined independently on each wavelength channel. The first equation in Eq. (10) relates to transmission $|\mu|$ not occupying wavelength a but another wavelength $b \neq a$; the second equation shows the if wavelength a is selected by message $|\mu|$, then other wavelength $b \neq a$ cannot be occupied; the third equation expresses that states $s \neq 0, \mu$ are not admissible. After introducing the auxiliary nodes, we treat the messages to and from them as to other network nodes. For example, the neighboring nodes set of node i in Fig. 2(a) is $\partial i = \{j, k, l, \mu\}$, and the calculation of messages $i \to j$ and $i \to \mu$

both follow Eq. (8). The marginal probability of edge (i, j) being in state s using wavelength a is then given by

$$\phi^a_{i,j}(0) = \psi^a_{i\to j}(0) + \psi^a_{j\to i}(0) + \min_n \left[F_{i,j}(n) + \min_{\substack{\sum_{b\neq a} s^b = n: \\ s^b=0,1}} \sum_{b\neq a} \tilde{\phi}^b_{i,j}(s^b) \right],$$

$$\phi^a_{i,j}(s) = \psi^a_{i\to j}(s) + \psi^a_{j\to i}(-s) + \min_n \left[F_{i,j}(n+1) + \min_{\substack{\sum_{b\neq a} s^b = n: \\ s^b=0,1}} \sum_{b\neq a} \tilde{\phi}^b_{i,j}(s^b) \right], \tag{11}$$

and the state $s^a_{i,j}$ of wavelength a of edge (i, j) is determined by

$$s^a_{i,j} = \arg\min_s \phi^a_{i,j}(s), \tag{12}$$

which ultimately leads to the optimized configuration of routes for all M transmissions through the optical network with Q wavelength channels.

1. Linear cost

While the objective function can take many different forms we use a simple power as the cost function $F_{i,j}(x)$ on edges x^γ [6,56], as it provides a good example of both concave and convex costs. When $\gamma = 1$, the cost function is linear and equivalent to the total length of all transmissions $L \equiv \sum_{(i,j);a} (1 - \delta^0_{s^a_{i,j}})$, and optimizing it is equivalent to finding the shortest average path.

In this case ($\gamma = 1$), the message-passing equations Eq. (8) can be simplified to

$$\phi^a_{i\to j}(0) = \min \left\{ \sum_{k\in\partial i\setminus j} \phi^a_{k\to j}(0),\ \min_{\substack{m,n\in\partial i\setminus j \\ s\neq 0}} \left[\phi^a_{m\to i}(s) + \phi^a_{n\to i}(-s) + \sum_{k\in\partial i\setminus j,m,n} \phi^a_{k\to i}(0) \right] \right\},$$

$$\phi^a_{i\to j}(s) = 1 + \min_{k\in\partial i\setminus j} \left[\phi^a_{k\to i}(s) + \sum_{l\in\partial i\setminus j,k} \phi^a_{l\to i}(0) \right], \tag{13}$$

where the variable ψ in Eq. (8) can be omitted. The marginal quantities are then given by

$$\phi^a_{i,j}(s) = \phi^a_{i\to j}(s) + \phi^a_{j\to i}(-s) + \left(\delta^0_s - 1\right), \tag{14}$$

and the messages to the auxiliary nodes at the origins and destinations are the same as Eq. (10).

2. Switching wavelength channels at nodes

A generalization of the NDP scenario is to allow for transmissions to change wavelengths at nodes (WS) as shown in Fig. 1(b), which is equivalent to a single-wavelength network routing with both node and edge capacity being Q, and utilize other multiplexing techniques than wavelength division (e.g., code or time division multiplexing). A variable τ is introduced to enforce this capacity constraint on nodes. In this case, the message-passing equations are given by

$$\phi^\mu_{i\to j}(0) = \min \left\{ \tau^\mu_i(0) + \sum_{k\in\partial i\setminus j} \phi^\mu_{k\to i}(0),\ \tau^\mu_i(1) + \min_{m,n\in\partial i\setminus j} \left[\phi^\mu_{m\to i}(1) + \phi^\mu_{n\to i}(-1) + \sum_{k\in\partial i\setminus j,m,n} \phi^\mu_{k\to i}(0) \right] \right\},$$

$$\phi^\mu_{i\to j}(\pm 1) = \tau^\mu_i(1) + 1 + \min_{k\in\partial i\setminus j} \left[\phi^\mu_{k\to i}(\pm 1) + \sum_{l\in\partial i\setminus j,k} \phi^\mu_{l\to i}(0) \right], \tag{15}$$

where τ^μ_i denotes the summation over $\tilde{\psi}_i$ from a total of at most Q transmissions, excluding μ, that pass through node i, given by

$$\tau^\mu_i(0) = \min_{\substack{\sum_{\nu\neq\mu} \sigma^\nu \leq Q_i \\ \nu\neq\mu:\sigma^\nu=0,1}} \sum_{\nu\neq\mu} \tilde{\psi}^\nu_i(\sigma^\nu), \quad \tau^\mu_i(1) = \min_{\substack{1+\sum_{\nu\neq\mu} \sigma^\nu \leq Q_i \\ \nu\neq\mu:\sigma^\nu=0,1}} \sum_{\nu\neq\mu} \tilde{\psi}^\nu_i(\sigma^\nu). \tag{16}$$

Specifically, $\tau^\mu_i(1)$ could be understood as indicating that there are free wavelength channels on i that μ could take, and $\tau^\mu_i(0)$ indicates that transmission μ does not pass through node i. The quantity $\tilde{\psi}^\mu_i$ is an auxiliary variable related to the probability that node i would be a part of the path of transmission μ, which leads to

$$\tilde{\psi}^\mu_i(0) = \sum_{j\in\partial i} \phi^\mu_{j\to i}(0), \quad \tilde{\psi}^\mu_i(1) = \min_{j,k\in\partial i} \left[\phi^\mu_{j\to i}(1) + \phi^\mu_{k\to i}(-1) + \sum_{l\in\partial i\setminus j,k} \phi^\mu_{l\to i}(0) \right]. \tag{17}$$

The messages from the origin and the destination of transmission μ to the neighboring edges are slightly different from the previous case of NDP without switching. In Eq. (16) $Q_i = Q$, and $\tilde{\psi}_i(1) = 0$ and $\tilde{\psi}(0) = \infty$ for the transmissions using node i as their origin or destination. Alternatively, one can set $Q_i = Q - M_i$, where M_i is the number of transmissions using node i as their origin or destination, and then exclude these transmissions when one calculates τ_i. Here, we first introduce a variable $\mu_i = \pm 1$ to denote node i as the origin or destination of transmission μ, respectively, given by

$$\phi^{\mu}_{i\to j}(0) = \min_{k\in\partial i\setminus j}\left[\phi^{\mu}_{k\to i}(-\mu_i) + \sum_{l\in\partial i\setminus j,k}\phi^{\mu}_{l\to i}(0)\right], \quad \phi^{\mu}_{i\to j}(\mu_i) = 1 + \sum_{k\in\partial i\setminus j}\phi^{\mu}_{k\to i}(0), \quad \phi^{\mu}_{i\to j}(-\mu_i) = \infty. \tag{18}$$

The variable $\phi^{\mu}_{i,j}$ determines the state of edge (i, j), i.e., whether it is a part of the path of transmission μ or not, and its expression is given by

$$\phi^{\mu}_{i,j}(\sigma) = \phi^{\mu}_{i\to j}(\sigma) + \phi^{\mu}_{j\to i}(-\sigma) + \left(\delta^0_{\sigma} - 1\right), \tag{19}$$

such that the optimized state is $\sigma^{\mu}_{i,j} = \arg\min_{\sigma}\phi^{\mu}_{i,j}(\sigma)$.

B. Edge-disjoint routing

Edge-disjoint path routing (EDP) is similar to NDP routing but is less restrictive, since nodes can accommodate any number of paths with the same wavelength but edges do not [11] [Fig. 1(c)]. In other words, for node i, if there exists an edge (i, j) with $s^a_{i,j} = s_0 \neq 0$, then there exists one and only one edge (i, k) with $s^a_{i,k} = -s_0$ continuity of transmission path, while other neighboring edges using *the same wavelength channel a* could be either in state 0 or take up other transmissions such that $s^a_{i,m_1} = -s^a_{i,n_1} = s_1 \neq 0$, $s^a_{i,m_2} = -s^a_{i,n_2} = s_2 \neq 0$ etc. In comparison, for NDP at most two variables $s^a_{i,j}$ for neighboring nodes $j \in \partial i$ can assume a nonzero value. In other words, single-wavelength EDP is equivalent to a generalized version of WS, where the capacity of each node is nonuniform and determined by its degree and the number of it being chosen as origins or destinations of transmissions. Consequently, the message passing equations for EDP scenarios are more complicated and their computational complexity is higher. The corresponding message passing equations are given by

$$\begin{aligned}
&\psi^a_{i\to j}(0) = \min_{\substack{\text{matched}\\ \text{pairs:}\vec{s}_{\partial i\setminus j}}}\sum_{k\in\partial i\setminus j}\phi^a_{k\to i}(s_k), \quad \psi^a_{i\to j}(s) = \min_{k\in\partial i\setminus j}\left[\phi^a_{k\to i}(s) + \min_{\substack{\text{matched}\\ \text{pairs:}\vec{s}_{\partial i\setminus j,k}}}\sum_{l\in\partial i\setminus j,k}\phi^a_{l\to i}(s_l)\right];\\
&\phi^a_{i\to j}(0) = \psi^a_{i\to j}(0) + \min_n\left[F_{i,j}(n) + \min_{\substack{\sum_{b\neq a}s^b=n:\\ s^b=0,1}}\sum_{b\neq a}\tilde{\phi}^b_{i,j}(s^b)\right], \quad \phi^a_{i\to j}(s) = \psi^a_{i\to j}(s) + \min_n\left[F_{i,j}(n+1) + \min_{\substack{\sum_{b\neq a}s^b=n:\\ s^b=0,1}}\sum_{b\neq a}\tilde{\phi}^b_{i,j}(s^b)\right],
\end{aligned} \tag{20}$$

where the message from node i to edge (i, j) (first two equations) are different from those of NDP in Eq. (8), while Eqs. (9)–(12) in the NDP scenario apply also here.

It is numerically difficult to compute the message passing relations in Eq. (20), since all feasible configurations satisfying the constraints have to be considered by the first two equations, which results in a computational complexity of

$$\sum_{n=0}^{\min\{\lfloor K/2\rfloor, M\}} {}^{M}C_n\ {}^{K}P_{2n}, \tag{21}$$

where $K = |\partial i| - 1$ is the number of neighboring edges of node i, M is the total number of transmissions, $\lfloor x\rfloor$ is the floor function that is equal to the greatest integer less than or equal to x, ${}^{n}P_k = \frac{n!}{(n-k)!}$ is the number of ordered permutations of k out of n elements and ${}^{n}C_k = \frac{n!}{k!(n-k)!}$ the number of unordered combinations. To simplify the computation we map the task on to the maximum weight matching problem [11,57]. As in Ref. [11], we consider all the possible pairs of considered edges $\{(i, k) \mid k \in \partial i \setminus j\}$ and obtain the weight of each pair,

$$w_{k,l} = -\min_{s=-M}^{M}[\phi_{k\to i}(s) + \phi_{l\to i}(-s)]. \tag{22}$$

Then, we construct a weighted graph with $|\partial i| - 1$ nodes where the weight of each edge is given by Eq. (22). After that, $\psi^a_{i\to j}$ in Eq. (20) could be obtained by the maximum weight matching algorithm [11,58].

In Fig. 3, we show the transformation employed for calculating the messages $i \to j$. Links between all pairs, including auxiliary origin-destination and graph edges, are shown on the left. The right figure shows all valid links between nodes, while distinguishing between auxiliary and graph nodes: Any of the ordinary graph nodes could be paired but the auxiliary nodes could only be paired with ordinary graph nodes. The maximum matching algorithm finds edge sets with the maximum sum of weights, where matched edges have no common nodes; the inverse value of the weights sum is approximately the value of minimum matched configurations in Eq. (20).

1. Linear cost

Similar to Sec. III A 1, if the cost function on edges is linear $F_{i,j}(x) = x$, then the message-passing equations could be simplified as follows:

$$\phi^a_{i\to j}(0) = \min_{\substack{\text{matched}\\ \text{pairs:}\bar{s}_{\partial i\setminus j}}} \sum_{k\in\partial i\setminus j} \phi^a_{k\to i}(s_k), \quad \phi^a_{i\to j}(s) = 1 + \min_{k\in\partial i\setminus j}\left[\phi^a_{k\to i}(s) + \min_{\substack{\text{matched}\\ \text{pairs:}\bar{s}_{\partial i\setminus j,k}}} \sum_{l\in\partial i\setminus j,k} \phi^a_{l\to i}(s_l)\right]. \tag{23}$$

The marginal states of nodes and edges, and messages to the auxiliary nodes at transmission origins and destinations, are the same as in the NDP case of Eqs. (10) and (14).

C. Algorithmic framework

The same algorithmic procedure governs both NDP and EDP routing algorithms based on the message passing equations. The min-sum algorithm, i.e., zero-temperature optimization algorithm, follows the process outlined below:

(1) initialize the messages $\{\psi^a_{i\to j}, \phi^a_{i\to j}, \phi_{\mu\to a}\}$ randomly (e.g., uniform distribution $U(-1, 1)$) or identically (e.g., all 1);

(2) update the messages by Eqs. (8)–(10) in the node-disjoint scenarios, and Eqs. (20) and (10) in the edge-disjoint scenarios until convergence or when a maximum number of iteration steps is reached;

(3) calculate the marginal state of edges by Eq. (11) and the state of each wavelength channel by Eq. (12).

After obtaining the marginal states of edges and wavelengths, the allocation of transmissions to specific wavelength and path would follow. Wavelength-edges $|s^a_{i,j}| = |\mu|$ construct the transmission-path $|\mu|$ with wavelength choices included.

However, there are some cases when the algorithms need many iterations to provide a valid configuration, for example if the cost function $F_{i,j}(x)$ in Eq. (1) is concave, e.g., $F(x) = \sqrt{x}$ in these cases, a decimation procedure can be introduced to speed up convergence. As an example, here we show the NDP algorithm with decimation (fixing states at intermediate steps) incorporated as part of the process:

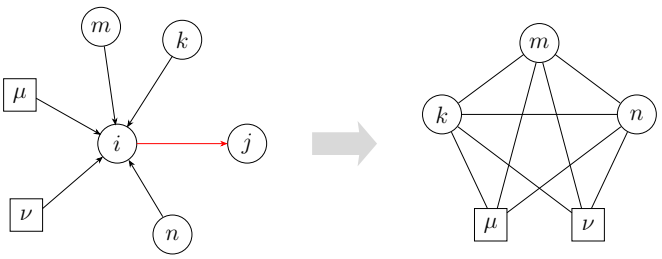

FIG. 3. Mapping from EDP to a maximum weighted matching graph. To calculate the message $\psi_{i\to j}$ by Eq. (20), we have to consider all valid paired configurations of neighboring nodes $\{k, m, n, \mu, \nu\}$. Transmissions could pass through $m \to i \to n$, so there is an edge (m, n) representing the pair interaction, and the contribution to $\phi_{i\to j}$ is approximately $\min_s[\phi_{m\to i}(s) + \phi_{n\to i}(-s)]$, whose inverse value is the weight of edge (m, n). Auxiliary (square) nodes μ and ν represent virtual origins or destinations of different transmissions so there are no paths of the form $\mu \to i \to \nu$, and consequently no edges between them exist.

(1) initialize the messages $\{\psi^a_{i\to j}, \phi^a_{i\to j}, \phi_{\mu\to a}\}$ and the state of all wavelength channels per available (undecimated) edge;

(2) update the messages of the available wavelength channels and edges by Eq. (8)–(10) for a specific number of iteration steps;

(3) compute the marginal states of the available wavelength channels and edges by Eq. (11); calculate the quantity $\hat{\phi}^a_{i,j} = \min_{s\neq 0} \phi^a_{i,j}(s) - \phi^a_{i,j}(0)$, and fix the state of the wavelength channel a of edge (i, j) with the largest value of $\hat{\phi}^a_{i,j}$ to be $s^a_{i,j} = 0$.

(4) iterate steps 2 and 3 and determine the state of the available wavelength channels and edges by Eq. (12) until a valid solution is obtained or a maximum number of iteration steps is reached.

The algorithms with or without the decimation procedures have a similar performance in terms of the optimized cost, but for harder problem (e.g., $F(x) = \sqrt{x}$) the decimation procedures can reduce the number of iteration steps needed for generating a valid routing solution.

As the problem becomes more challenging, e.g., larger M, Q or N, the number of iteration required for the iterative process to converge grows as demonstrated in the inset of Fig. 14(a). To mitigate the increase in computation we employ a commonly used heuristic, a reinforcement term [11], shown to reduce the number of iterations required. We first generalize the marginal Eq. (14) to

$$\phi^a_{i,j}(s) = \phi^a_{i\to j}(s) + \phi^a_{j\to i}(-s) - \tilde{w}^a_{i,j}(s), \tag{24}$$

and update the local fields at each iteration by

$$\tilde{w}^a_{i,j}(s) \leftarrow \tilde{w}^a_{i,j}(s) + \varepsilon\phi^a_{i,j}(s), \tag{25}$$

where ε is the reinforcement factor, which can take a positive small constant (e.g., 10^{-4}), or a slowly increasing value.

Due to the hard computational nature of the problem, it is expected that the algorithm will fail in specific instances, which is exacerbated as the problem becomes more difficult, beyond some critical ratio between constraints and free variables or form of objective function. Moreover, while decimation and reinforcement tend to speed up convergence they typically increase the failure rate, driving the dynamics towards suboptimal and invalid solutions. To study the impact of decimation and reinforcement on the quality of the results obtained and the failure to obtain solutions, we carried out a set of experiments below the experimental capacity as reported in Table I. It shows that below the capacity limit almost all instances converge to valid solutions, with the exception of the concave objective $F(x) = \sqrt{x}$, where a low

TABLE I. The number of iterations and success rates of three versions of the message-passing algorithm: Original algorithm with no heuristics (MP), with decimation (MPD), and with reinforcement procedures (MPR). The experiments were carried out for EDP routing and objective functions of the form $F(x) = x^{\gamma}$: Concave ($\gamma = 0.5$), linear ($\gamma = 1$), and convex ($\gamma = 2$) costs. Results are obtained by 36 testing samples on network CONUS below the critical capacity with $Q = 4$ wavelengths, $M = 18$ communication requests, and up to 10^5 iterations. It is clear that the concave case is the most difficult, and that in the selected example decimation and reinforcement terms are useful.

γ	0.5			1			2		
Methods	MP	MPD	MPR	MP	MPD	MPR	MP	MPD	MPR
Avg (iteration)	20806	1959.4	79.4	350.7	557.3	62.6	114.6	117.6	84.1
Std (iteration)	22667	639.5	20.3	1002.8	947.9	21.7	33.3	58.7	26.9
Success rate	36.11%	100%	100%	100%	100%	100%	100%	100%	100%

percentage of instances converge for the original algorithm; message-passing with decimation or reinforcement helps in increasing performance and convergence rates. All three versions of message passing have higher failing probabilities as the task becomes more difficult, for instance, increasing the number of requests M or lowering the number of wavelengths Q, requiring additional iterations or more trials from different initial conditions to obtain valid solutions.

IV. SIMULATION RESULTS

A. Linear cost

We first examine the NDP, WS, and EDP scenarios with linear cost $F(x) = x$ to explore the behavior and performance of communication networks, such as capacity and average length, with impact on latency and number of wavelength channels required.

1. Dependence on the number of wavelength channels

We performed numerical experiments using the three algorithms on three different types of generated random networks, each of which has a single connected component, including random regular graphs, Erdős-Rényi and scale-free networks with 100 nodes and an average node degree of 3, as well as on two real optical communication networks—CONUS60, which has 60 nodes and 79 edges [46] and BT-Core, 22 nodes, and 35 edges [45] as shown in Fig. 4. Specifically, for the scale-free networks studied, the degree distribution is $p(d) \propto d^{-1.24}$.

We define the *capacity* to be the maximum number of transmissions, which we denote as $M_{\max}$, that can be transmitted by an optical communication network with Q wavelength channels. We remark that capacity depends on network topologies and the set of origin-destination pairs, so in Fig. 5 we report the dependence of the average value of $M_{\max}$ with standard deviation as error-bars on Q, showing the average behavior of capacities for different Q values.

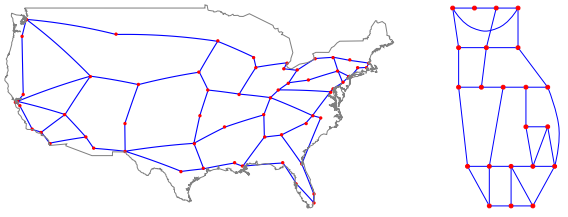

(a) CONUS (b) BT-Core

FIG. 4. Real optical communication networks studied, namely, (a) CONUS60 in the United States, and (b) BT-core in the United Kingdom.

Figure 5 shows the simulation results for the five types of networks—in the three different routing scenarios. For the three types of random networks and BT-Core, the average capacity per wavelength channel $M_{\max}/Q$ keeps increasing at the beginning and become saturated as the number of wavelength channels Q increases. As for the networks CONUS and BT-Core in Fig. 5, we see that the average capacities also increase with Q but the increases are not as fast as that in the generated networks. Random regular networks are the most homogeneous among the three types of generated networks and scale-free the most heterogeneous, which explains why random regular networks have higher capacity than Erdős-Rényi networks and scale-free networks are more likely to be blocked [59].

The average path length of the corresponding networks are shown in Figs. 6 and 7. In Fig. 6, we see that as more wavelengths are available the shorter the average path length L/M decreases; for instance, in NDP scenarios shown in Figs. 6(a)–6(c), the average path length with $Q = 1$ is higher than that with $Q = 4$, which is higher than that of $Q = 9$ as the average load per wavelength channel (M/Q) increases. Moreover, with the same values of Q and M, it is clear that the wavelength-switching model would provide us with shorter paths and a higher capacity on Erdős-Rényi and scale-free networks as shown in Fig. 6.

In comparison with NDP, the advantages of EDP with multiple transmissions using the same wavelength availability is clearer on random regular graphs as shown in Fig. 7(a), and less so on other graph types, presumably due to the graph heterogeneity and finite size effects. We observe that EDP routing increases the network capacity, i.e., average transmission load per wavelength channel, and provides shorter valid paths.

2. Dependence on the number of transmissions

In practice, one may wish to minimize the total number of active wavelength channels for given demand. We define the smallest number of wavelength channels which accommodate a set of transmission to be $Q_{\min}$; to find $Q_{\min}$ for a specific instance, we gradually increase Q from 1 until a valid solution is found by the algorithms. Here we compare the results of $Q_{\min}$ obtained by our proposed multiwavelength

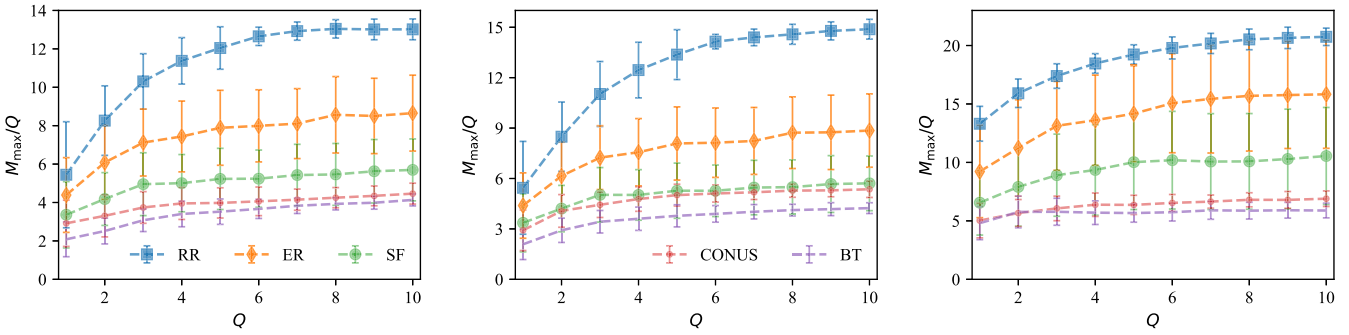

(a) Node-disjoint (b) Node-disjoint wavelength-switching (c) Edge-disjoint

FIG. 5. The capacity per wavelength channel, i.e., M_{max}/Q, as a function of Q, in the NDP, wavelength-switching and EDP scenarios with linear cost, on random regular (RR), Erdős-Rényi (ER), and scale-free (SF) networks, as well as a real optical communication networks known as CONUS and BT [45,46]. All three types of generated networks have 100 nodes and an average degree of 3, while the CONUS network has 60 node and 79 edges, and BT 22 nodes and 35 edges. All the results are obtained by averaging 36 realizations.

routing (MWR) algorithms to those obtained by a multitrial greedy assignment (MGA) algorithm in the node-disjoint or edge-disjoint scenarios following the process outlined below:

(1) initialize the values of ΔM, M, Q, and M_*, where M to M_* represent the range of transmission number values we want to explore and ΔM the step size increase in the experiment;

(2) read the first M elements of the random origin-destination pair list, set $Q = \max(1,\ Q-4)$ to increase the probability of finding a solution in the case of small Q;

(3) randomly assign the M transmissions into Q wavelength channels, and solve the routing problem for each transmission on the individually assigned wavelength channel separately;

(4) repeat step 3 up to a maximum number of trials (e.g., 10) until a valid configuration is found;

(5) if step 4 fails, set $Q := Q+1$ and repeat until a valid configuration is obtained, then the value of Q is the smallest number of wavelengths Q_{min} that accommodates the M transmissions;

(6) increase $M := M + \Delta M$ and repeat steps 2–5 until $M \geqslant M_*$.

We compare the values of Q_{min}/M obtained by our algorithms and by the MGA algorithm on random regular networks, the CONUS and BT-Core networks, in both NDP and EDP scenarios. The numerical results on random regular

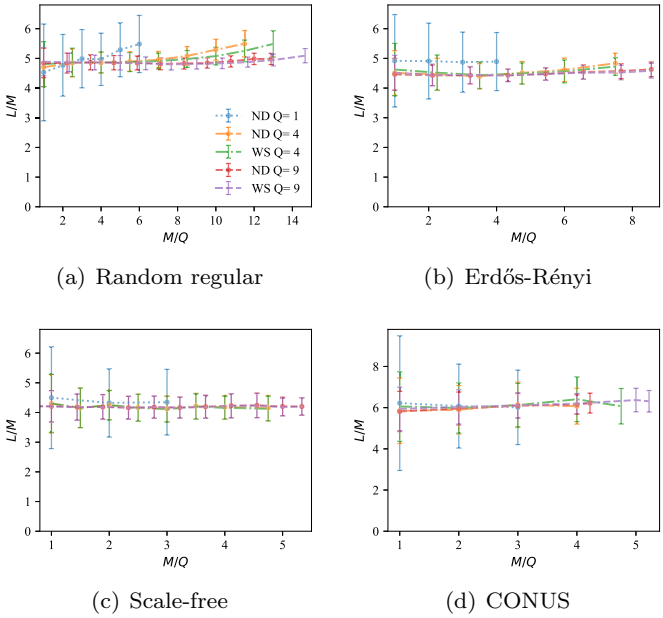

(a) Random regular (b) Erdős-Rényi

(c) Scale-free (d) CONUS

FIG. 6. The dependence of the path length L/M on the number of transmissions per wavelength M/Q for different Q values, in the NDP and wavelength-switching (WS) scenarios with a linear cost, and for the four types of graphs studied. The results are obtained by averaging no less than 20 samples. The WS scenario does not show a significant advantage over the original node-disjoint scenario for Erdős-Rényi networks based on the limited simulation results.

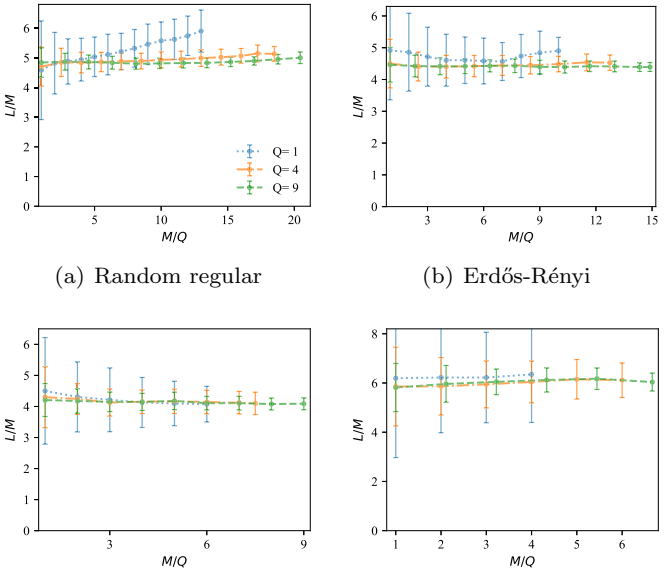

(a) Random regular (b) Erdős-Rényi

(c) Scale-free (d) CONUS

FIG. 7. The dependence of the path length L/M on the number of transmissions per wavelength M/Q for different values of Q, in EDP scenarios with a linear cost, and for the four types of graphs studied. The results are obtained by averaging no less than 20 samples per point.

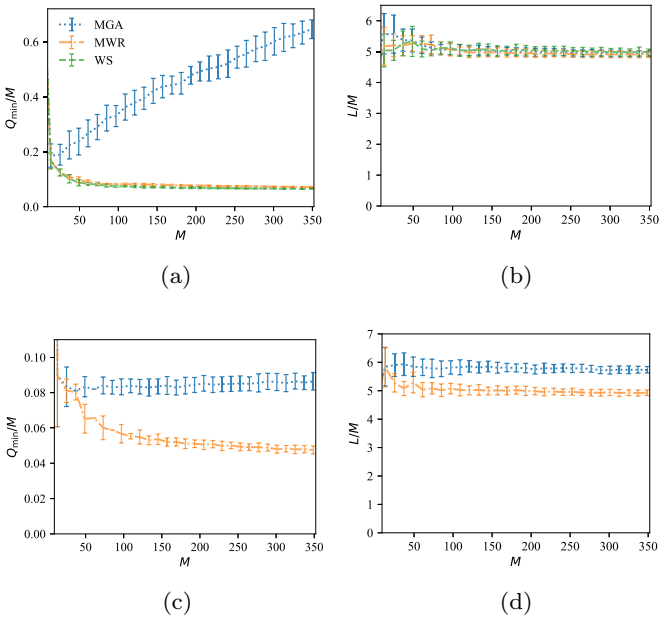

FIG. 8. The average smallest number of wavelength channels $Q_{\min}/M$ with (a) NDP and (c) EDP routing, and the average path length with (b) NDP and (d) EDP routing, as a function of the number of transmissions M, on random regular networks with 100 nodes and degree 3, obtained by our multiwavelength routing algorithm with NDP/EDP (MWR, orange) and WS (green), in comparison with the multitrial greedy assignment algorithm (MGA, blue). The results are obtained by averaging 36 samples.

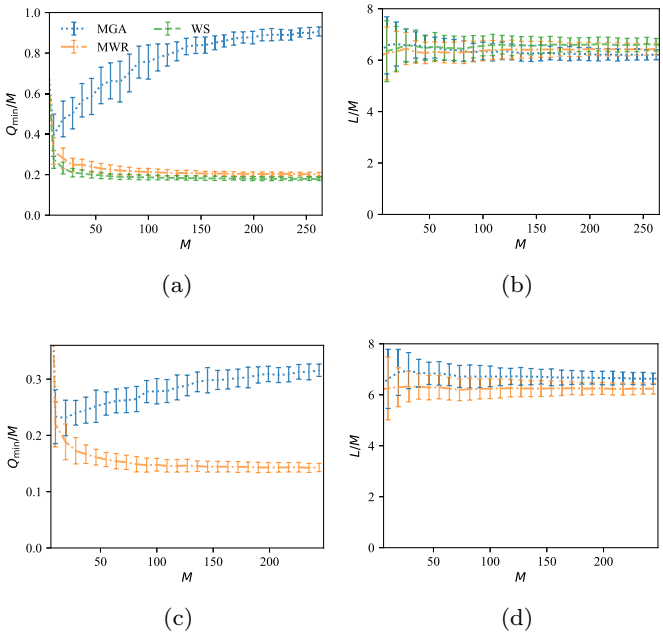

FIG. 9. The average smallest number of wavelength channels $Q_{\min}/M$ with (a) NDP and (c) EDP routing, and the total path length with (b) NDP and (d) EDP routing, as a function of the number of transmissions M, on the CONUS network, obtained by our MWR algorithm with NDP/EDP (orange) and WS (green), in comparison with MGA algorithm (blue). The results are obtained by averaging 36 samples.

networks presented in Figs. 8(a) and 8(c) show that our algorithms offer significant advantages over the MGA algorithm in reducing the number of wavelength channels required for specific random transmission pairs in. The improved performance is also observed on the CONUS and BT-Core networks in Figs. 9 and 10, respectively. The underlying reason for the improvement is the low success rate of random greedy assignments. The numerical results demonstrate that our MWR algorithms lead to a better use of resource. The additional flexibility provided by the wavelength-switching on transceivers leads to an even smaller value of $Q_{\min}$ as M increases in Figs. 8(a) and 9(a), whereas the experiments on the BT-Core network do not show a significant improvement of WS over the ordinary NDP in Fig. 10(a), which may depend on the topology of the graph or our range of values tested.

Comparing the average path length found for both NDP and EDP routing on random regular graphs, we see in Fig. 8(b) that the average path lengths obtained by the MGA and MWR for NDP routing are similar but that shorter paths are found by MWR in the EDP scenario [Fig. 8(d)]. A significant reduction in average route length is not expected since typical route lengths on random graphss is $O(\log N)$ with little variability. However, a significant reduction in the number of wavelength channels used $Q_{\min}$, is shown in Fig. 8(d) and a similar trend is shown for EDP scenarios in Figs. 9(a), 9(c) and 10(a), 10(c) for the two real networks.

3. Network capacity

The results of $M_{\max}(Q)$ or $Q_{\min}(M)$ shown in the previous two subsections point to the existence of a maximum capacity for individual optical communication networks, i.e., the maximum number of transmissions accommodated by a specific number of wavelength channels and topology. Nevertheless, these estimates of maximum capacity can be inaccurate if our MWR algorithm fails to identify existing path solutions, especially since it can be difficult to find these solutions when the networks are working close to their maximum capacity. To show that our algorithm is effective even in this algorithmic-hard regime, we cross-validate the results of $M_{\max}(Q)$ and $Q_{\min}(M)$ by showing both dependencies on the same graph, i.e., $M_{\max}(Q)$ and the inverse $Q^{-1}_{\min}(M)$ in Fig. 11. As we can see, $M_{\max}(Q)$ and $Q^{-1}_{\min}(M)$ found by our algorithm are in good agreement for random regular graphs, the CONUS and the BT-core network in all three studied scenarios NDP, WS, and EDP. These results show the efficacy of our MWR algorithm in identifying solutions when the networks are close to their maximum capacity, as well as its efficacy in identifying the intrinsic capacities of optical communication networks such as the CONUS and BT-core networks.

B. Computational complexity

Next, we discuss the computational complexity of our multiwavelength routing algorithms with a linear cost function $F_{i,j}(x) = x$. In this case, if we use the normalization $\phi^a_{i\to j}(s) := \phi^a_{i\to j}(s) - \phi^a_{i\to j}(0)$ in the min-sum Eqs. (13), (15), and (20), the computational complexities would decrease.

Under NDP routing, the complexity in computing Eq. (13) is approximately $O(\langle k\rangle^2 M)$, where $\langle k\rangle$ is the average node degree, and there are $\langle k\rangle NQ$ such messages. The complexity

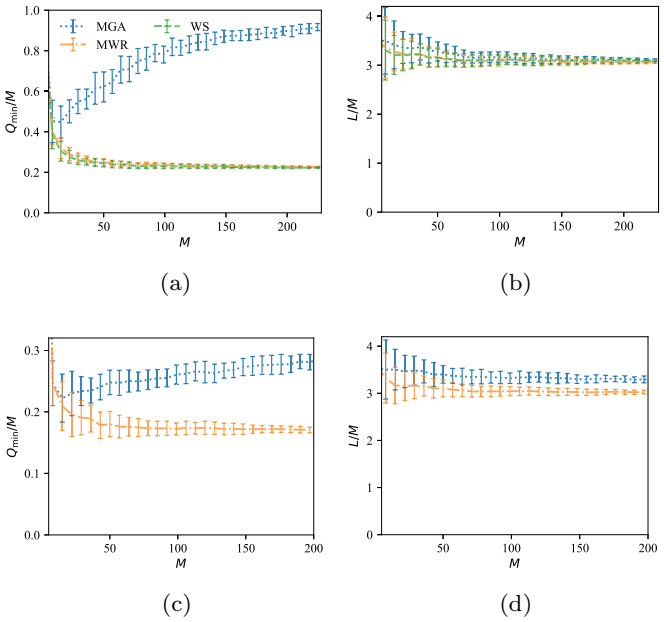

FIG. 10. The average smallest number of wavelength channels $Q_{\min}/M$ with (a) NDP and (c) EDP routing, and the total path length with (b) NDP and (d) EDP routing, as a function of the number of transmissions M, on the BT-core network, obtained by our MWR algorithm with NDP/EDP (orange) and WS (green), in comparison with MGA algorithm (blue). The results are obtained by averaging 36 samples.

in computing the messages from origin and destination nodes in Eq. (10) is $O(Q)$, and there are $2MQ$ such messages. Therefore, the total complexity of one round of update for all messages is $O(\langle k\rangle^3 MNQ + MQ^2)$; if the graph is sparse, i.e., $\langle k\rangle \ll N$, the complexity becomes $O(MNQ + MQ^2)$. For large graphs and relatively small $Q \ll N$, the complexity is roughly $O(MNQ)$, which linearly scales with Q as shown in Fig. 12(a).

For EDP routing, the complexity of matching a pair of incoming and outgoing transmissions with the same wavelength in Eq. (23) is $O(\langle k\rangle^3 \log\langle k\rangle)$ [11]. Therefore, the total complexity of one round of update for all messages is $O(2M\langle k\rangle^4 \log\langle k\rangle \times \langle k\rangle NQ + MQ^2)$, and if the graph is sparse the complexity becomes $O(MNQ + MQ^2)$. For relatively small Q, the complexity scales with Q as in NDP routing as shown in Fig. 12(b).

However, when $M/N \ll N$, the effective degree becomes quite different from the average degree $\langle k\rangle \Rightarrow \langle k\rangle + \frac{2M}{N}$ [see in Fig. 2(a), the degree of node i increases from 3 to 4 after introducing the auxiliary node μ]. When M is very large, for instance $M \sim O(N^2)$ as is used in many optical communication network applications, the effect of effective degree cannot be omitted. To make the algorithm scale better we divide the messages into three types:

(1) messages from auxiliary nodes to ordinary nodes, e.g., $\mu \to i$ in Fig. 2(a)—there are $2MQ$ such messages;

(2) messages from ordinary nodes to ordinary nodes, e.g., $i \to j$ in Fig. 2(a)—there are $\langle k\rangle NQ$ messages of this type;

(3) messages from ordinary nodes to auxiliary nodes, e.g., $i \to \mu$ in Fig. 2(a)—there are also $2MQ$ such entities.

The messages of type 1 obeys Eq. (10) and the resulting total complexity is $O(MQ^2)$.

Noticing that the messages from auxiliary nodes are sparse, only $\phi_{\mu\to a}(0)$ and $\phi_{\mu\to a}(\mu)$ are nontrivial in Eq. (10), and only $\phi_{b\to\mu}(-\mu)$ is needed to generate new messages, which simplifies the calculations of Eq. (13). Under NDP routing, by separating messages of type 1 and 2, the computational complexity of generating one message of type 2 or 3 by Eq. (13) is $O(\langle k\rangle^2 M)$. Then, the total complexity of the three types of messages is $O[MQ^2 + \langle k\rangle^2 M(\langle k\rangle NQ + MQ)] = O[MQ(M + N + Q)]$. Considering all possible pairs $M = N(N-1)/2$ and set $Q \sim O(N)$, the overall complexity becomes $O(N^5)$. In Fig. 12(c), we present the one-iteration computing time on random regular graphs with degree $k = 3$ and N nodes, the one-iteration computing timescales approximately as $N^{5.14}$, which fits our analysis of N^5. If $M/N \ll N$, then the complexity reduces to $O[MQ(N + Q)]$, which is equivalent to the previous estimate of $O(MNQ + MQ^2)$.

Under EDP routing, the computational complexity of type 2 and 3 messages depends on the complexity of the maximum weighted matching algorithm (approximately $O[(\langle k\rangle + \frac{2M}{N})^\alpha]$ with α being a coefficient to be determined. Using the sparse properties of type 1 and 3 messages, the total complexity of the three types is $O\{MQ[N + Q + (M/N)^\alpha]\}$. Recalling the mapping to matching problems—the matching network has approximately $\langle k\rangle + \frac{2M}{N}$ nodes and $\langle k\rangle(\frac{\langle k\rangle - 1}{2} + \frac{2M}{N})$ edges, and the average node degree is approximately $\langle k\rangle$ when $\frac{2M}{N} \gg \langle k\rangle$, therefore it is a sparse network. By using the algorithm in Ref. [11], the complexity should be approximately $O[(\langle k\rangle + \frac{2M}{N})^2]$. However, due to resulting topology and the special network structure our tests result in complexity scaling close to $O(\langle k\rangle + \frac{2M}{N})$. In other words, $\alpha = 1$ and therefore the resulting total complexity is $O[MQ(N + Q + M/N)]$. Experiments on random regular graphs presented in Fig. 12(c), when $M = N(N-1)/2$ and $Q = N$ show that the complexity is approximately $O(N^{3.92})$ which agrees well with the analysis of $O(N^4) = O(MNQ)$.

C. Nonlinear cost

In this section, we show the simulation results where a more general form of the cost function $F_{i,j}(x_{i,j}) = x_{i,j}^\gamma$, where the argument is the wavelength occupancy $q_{i,j}$ on edge (i, j), given by

$$x_{i,j} = \sum_{a=1}^{Q} \left(1 - \delta^0_{s^a_{i,j}}\right). \tag{26}$$

When $\gamma > 1$, the utility increases faster on heavily loaded edges, biasing solutions towards edges with more even loads. As a result, load variability on edges is reduced by having a smaller fraction of idle edges and by suppressing the tail of highly loaded edges, thus increasing intermediate-valued loads (e.g., convex cost—$\gamma = 2$). However, when $0 < \gamma < 1$, the cost on edges increases slower with the load, leading to configurations which consolidate transmissions on used edges, leaving more edges and wavelength channels idle. A concave cost reduces the number of active edges while increasing the load of nonidle edges (e.g., concave cost—$\gamma = 0.5$) and thus reducing the fraction of intermediate-

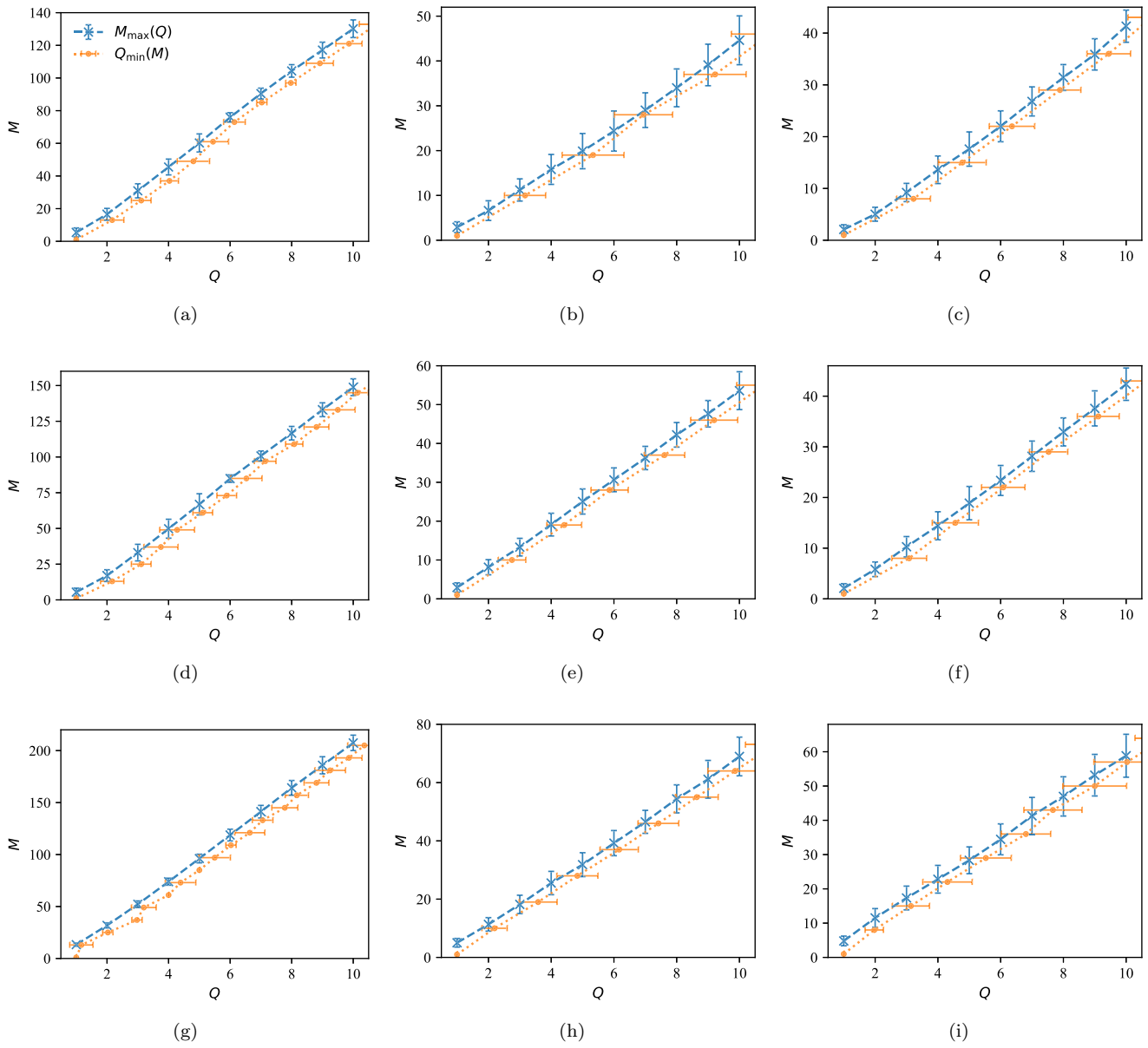

FIG. 11. Network capacity by cross-validating the results of $M_{max}(Q)$ and the inverse $Q_{min}^{-1}(M)$ obtained by our MWR algorithm for random regular graphs (a), (d), (g), the CONUS (b), (e), (h) and the BT-core (c), (f), (i) network in the three studied scenarios (a), (b), (c) NDP, (d), (e), (f) WS, and (g), (h), (i) EDP.

valued loads. It is relevant for identifying less important transceiver nodes which can be switched off in hours of low usage.

In Fig. 13 we show the distribution $p(x)$ of wavelength occupancy on edges of random regular graphs and the two real network CONUS and BT-Core for different values of γ. For all three networks and both NDP and EDP scenarios, we observe that when $\gamma = 0.5$ more edges were unused, i.e., a higher value at $p(x = 0)$ in Fig. 13, and as γ increases the distribution become more evenly distributed and peaked at some values of x, which corresponds to the balancing of edge loads. We show in the insets the relative difference between $p(x)$ obtained by $\gamma = 1$ and those obtained by $\gamma = 0.5$ or 2, i.e., $\delta(x;\gamma) \equiv \frac{p(x;\gamma)-p(x;\gamma=1)}{p(x;\gamma=1)}$, where the evidence for load consolidation or balancing, for $\gamma = 0.5$ or 2, respectively, become obvious.

D. Comparison with linear programming

Many variants of the RWA problem exist, addressing both static and dynamics scenarios, with the latter focusing on a greedy optimization of the most recently introduced request. We concentrate here on the static problem where all requests are optimized simultaneously, which can be easily converted into a version that optimizes only a set of new requests. In spite of its computational cost and mainly due to being a principled algorithm, integer linear programming (ILP) is regarded as the gold standard algorithm for throughput

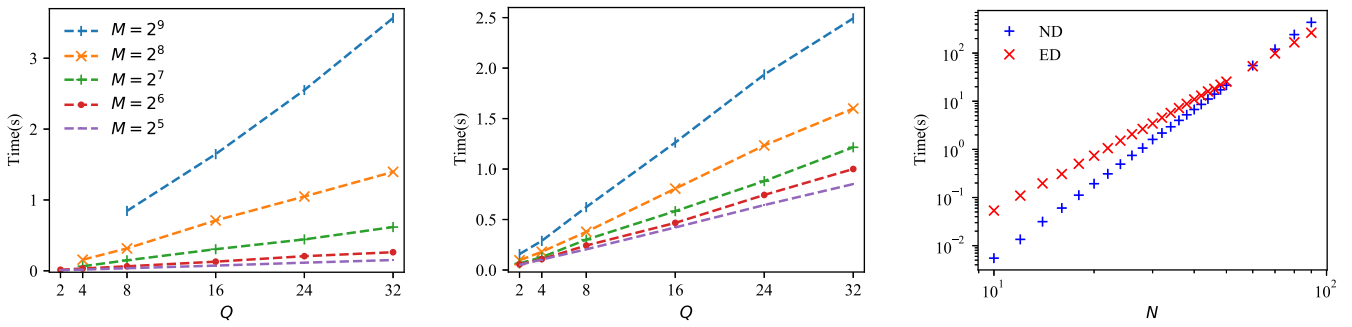

(a) Node-disjoint (b) Edge-disjoint (c) Large M complexity

FIG. 12. The dependence of one round of computational time costs from our multiwavelength routing algorithms on the number of wavelengths Q. For relatively small $Q \ll N$ and $M \ll N^2$, data obtained on random regular networks with 1000 nodes and degree 3 in (a) NDP and (b) EDP scenarios. With the same number of transmissions M, the time costs scale roughly linearly with Q for both scenarios. For large M, when allocate all the $M = N(N-1)/2$ transmissions on $Q = N$ wavelengths, the log-log plots of one round computation time and node size N are presented in panel (c). It is easy to draw straight lines to fit the data points and the fitting slops are around 3.92 and 5.14 for EDP and NDP scenarios, respectively. The simulations are implemented on random regular networks of degree 3 and node size N.

optimization in optical networks [2–4,60,61] and the one to compare against, not necessarily due to its speed but due to its ability to provide accurate results. Many (meta)heuristic algorithms have been proposed for solving the static RWA problem, for instance [62–65], and are all compared against integer linear programming (ILP) methods on small networks. Hence, we compare the results of our proposed algorithm with those obtained by linear programming with a linear cost function $\gamma = 1$.

To solve the routing problem using linear programming, we find n shortest paths for each of the M transmissions, denoted by the variables $\{\vec{s}_k^{\mu}\}$ with superscript $\mu = 1, \ldots, M$ representing transmissions and subscript $k = 1, \ldots, n$ representing the k^{th} candidate path for transmission μ. By carrying either a subscript for nodes or edges, the variables $\vec{s}_k^{\mu}$ can represent a configuration of node states or edge states, and the NDP or EDP constraints can both be expressed in terms of $\vec{s}_k^{\mu}$. In this case, we introduce a variable $\sigma_k^{a,\mu} = 1$ to denote that transmission μ chooses its k^{th} path with wavelength a, $\sigma_k^{a,\mu} = 0$ otherwise. The disjoint constraint can be expressed as follows:

$$\forall a, j: \quad v_j^a \leqslant 1, \text{ where } \vec{v}^a = \sum_{k,\mu} \sigma_k^{a,\mu} \vec{s}_k^{\mu}. \tag{27}$$

In Eq. (27), if the path $\vec{s}_k^{\mu}$ represents a configuration of node states, then each element of $\vec{v}^a$ represents the load of a^{th} wavelength channel on that node, and node-disjoint constraint restricts the value of the load to be no more than 1; if the path $\vec{s}_k^{\mu}$ represents a configuration of edges, then the edge-disjoint constraints can be defined in a similar manner.

For each transmission, we choose one wavelength to accommodate one candidate path, which is given by

$$\sum_{a,k} \sigma_k^{a,\mu} = 1, \ \forall \mu = 1, \ldots, M. \tag{28}$$

The objective function for the problem with linear cost is given by

$$\text{Minimize} \sum_{a,j} v_j^a. \tag{29}$$

The problem can be solved by linear programming with the objective function of Eq. (29) subject to the constraints in Eq. (27) and (28) where all the expressions are linear.

For the WS scenario, the variables σ_k^{μ} are introduced instead of the previous $\sigma_k^{a,\mu}$, and the capacity constraint for each node is given by

$$\forall j: \quad v_j \leqslant Q, \text{ where } \vec{v} = \sum_{\mu} \sigma_k^{\mu} \vec{s}_k^{\mu}, \tag{30}$$

where $\vec{s}_k^{\mu}$ is a configuration of node states. The constraint for all the transmissions is given by

$$\sum_{k} \sigma_k^{\mu} = 1, \ \forall \mu = 1, \ldots, M. \tag{31}$$

The objective function to be minimized is $\sum_j v_j$.

We conducted numerical experiments on four real-world networks [45,66–68] and compared the results obtained by our algorithms and linear programming in the NDP, wavelength-switching and EDP scenarios. A commonly used and well studied ILP solver, "intlinprog"—MATLAB mixed-integer linear programming solver—was used in these experiments. We show the smallest number of wavelength channels needed to route successfully all possible transmissions, $Q_{\min}$, and the corresponding total path length L in Table II. Our message-passing algorithms and linear programming yield almost identical performance in finding optimized path solutions. For relatively small network, linear programming is efficient, but it quickly becomes impractical as the size of networks increases, whereas we show in Sec. IV B that our message-passing algorithms have more practical scaling properties, both in terms of the operations per iteration and overall running time (Fig. 14).

E. Comparison with routing heuristics

There is a difficulty in comparing our results with state-of-the-art heuristics since most of the heuristics used in practice are highly suboptimal and are based on greedy shortest-path optimization, tailored to address the *practical* considerations of routing, such as the dynamical addition and deletion

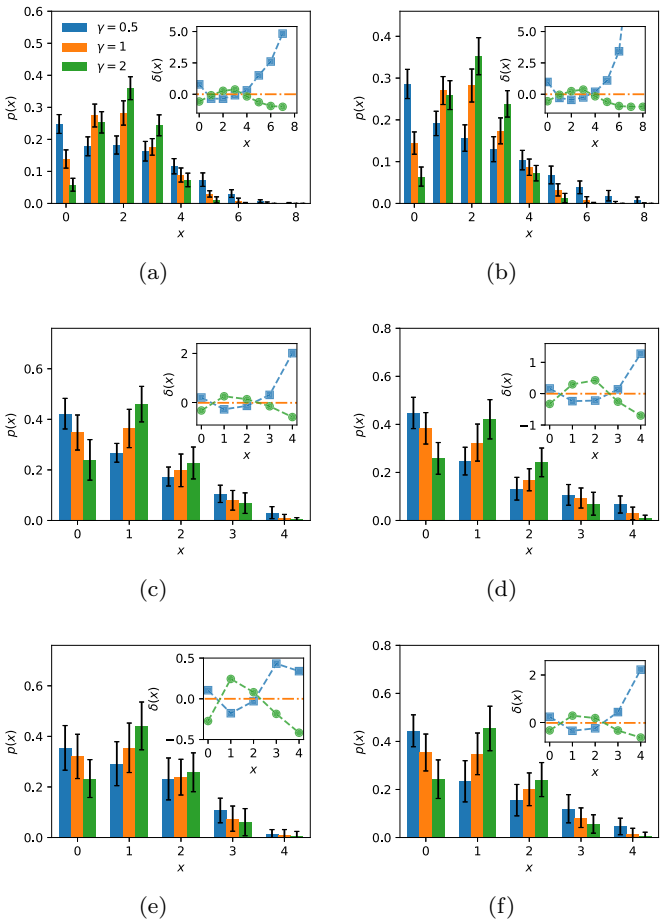

FIG. 13. The distribution $p(x)$ of wavelength occupancy on edges for power $\gamma = 0.5, 1, 2$ in the objective function; panels (a), (c), (e) represent NDP scenarios and panels (b), (d), (f) represent EDP scenarios for different graphs: (a), (b) random regular networks with 100 nodes, degree 3, $M = 60$ and $Q = 8$; (c), (d) the real network CONUS with $M = 14$ and $Q = 4$, and (e), (f) the BT-Core network with $M = 12$ and $Q = 4$. Insets: The relative difference $\delta(x; \gamma)$ between $\gamma = 0.5$ and 1, as well as between $\gamma = 2$ and 1. The results are obtained by averaging 22–36 realizations.

of requests, reducing lightpath changes, etc. Nevertheless, we compare the results obtained by our algorithm against those achieved by three commonly used RWA heuristics: The k-shortest-path first fit (kSP-FF), first fit k-shortest-path (FF-kSP) and adaptive shortest-path (ASP) algorithms [2–4,69]. Unlike our proposed message-passing method and ILP, the first two heuristics carry out the optimization using two separate steps: Routing and wavelength assignment. The kSP-FF algorithm aims to assign the shortest path from the k candidates followed by the wavelength assignment from the available ones (shorter path length precedes the wavelength assignment), whereas FF-kSP allocates the first available wavelength prior to routing optimization, based on shortest weighted path length among the k candidates; the ASP algorithm aims at finding the shortest path according to the *current* network state (similar to kSP-FF, where k corresponds to all paths). The numerical results presented in Fig. 15 show that message-passing outperforms these three heuristics: It offers higher success rates in allocating EDP paths to communication requests (higher throughput, lower blocking by invalid paths) and shorter average path lengths. Average path lengths are calculated with respect to communication requests *for which a solution has been found*, they are not expected to be significantly different since in unweighted networks they are dominated by the typical path length, which is $O(\log N)$. The figure is also slightly misleading, showing the kSP-FF algorithm to provide the shortest path length; this is an artifact of the low number of valid solutions found (about 30%–60% less than the other methods, failing on most of the more challenging and longer lightpaths).

TABLE II. The smallest number of wavelength channels $Q_{\min}$ required to transmit all $M = |V|(|V| - 1)/2 (= N(N - 1)/2)$ transmissions on four small real optical communication networks including NSF-Net, B4, DTAG/T-systems, and BT-Core, obtained by our multiwavelength message-passing routing algorithm (MP) compared to that obtained by linear programming (LP), in edge-disjoint (ED), node-disjoint (ND), and node-disjoint wavelength-switching (WS) scenarios. The corresponding total path lengths are also shown.

Network		NSF-Net	B4	DTAG/T-systems	BT-Core
$\|V\|$		14	12	14	22
$\|E\|$		21	19	23	35
M		91	66	91	231
MP-ED	$Q_{\min}$	13	16	14	39
	L	195	153	218	697
LP-ED	$Q_{\min}$	13	16	14	39
	L	195	153	218	697
MP-ND	$Q_{\min}$	25	23	29	52
	L	202	154	221	707
LP-ND	$Q_{\min}$	25	23	29	52
	L	201	154	221	709
MP-WS	$Q_{\min}$	25	23	29	51
	L	201	154	221	715
LP-WS	$Q_{\min}$	25	23	29	51
	L	201	154	221	715

V. GENERALIZATION TO HETEROGENEOUS EDGE WEIGHT AND WAVELENGTH AVAILABILITY

The presentation has so far focused on benchmark topologies, including some realistic networks, and generic traffic patterns. This has been done to provide a clear and controllable setup such that the scaling properties and performance of our algorithms could be demonstrated. In the absence of principled scalable competing algorithms, we compared the results obtained against the commonly used linear programming techniques that are applicable to small networks. However, routing in realistic networks is much more involved; methods and results vary between the different types of networks (e.g., data centers, backbone, and metropolitan networks) and include many practical parameters, considerations and implementation protocols that make the results and comparison less transparent.

Utilizing any new routing algorithm in a realistic network with dynamic traffic patterns includes a variety of practical considerations, such as variable availability of wavelengths per edge, routing only new requests that are raised within a

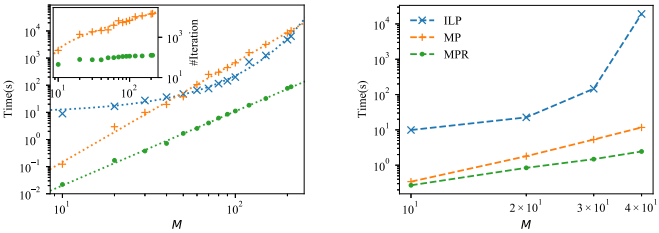

(a) NDP (b) EDP

FIG. 14. Real time routing costs on the network CONUS under NDP and EDP constraints using ILP and two versions of the message-passing algorithm. (a) NDP scenario, where the number of wavelengths Q grows linearly with the number of requests M according to $Q = 0.4M + 1$, to make sure solutions can be found. Solutions were obtained using the mixed-integer linear programming solver "intlinprog" from MATLAB R2019 (ILP), original message-passing algorithm (MP) and message-passing with reinforcement (MPR). The dotted curves are the corresponding fitting functions: ILP points are fitted well by the exponential function $9.27e^{0.0319M}$ (blue dotted curve), whereas the message-passing results are fitted by power functions, with approximate powers of $M^{3.27}$ and $M^{2.73}$ for MP and MPR, respectively. Inset: The number of iterations needed to generate solutions grows linearly as M increases for basic MP (fitting the orange dotted curve), whereas the reinforcement reduces iteration numbers significantly making it more computationally efficient, e.g., 40–130 in this example. (b) EDP scenario, under the same M range and the smallest Q which allows for the routing and wavelength assignment; the problem is more difficult than (a) and the time required is significantly longer. It is clear that even for relatively small M values the average running time for ILP to find solution grows quickly as M increases, way beyond what is needed in panel (a). However, the two versions of the message passing algorithm MP and MPR increase according to a power law as in panel (a). The results were obtained by averaging 10 samples. All the experiments, ILP by MATLAB and MPs by C++, were carried out on single CPU cores of the same platform, and the type of processor is Intel Xeon CPU E5-4620 0 @ 2.20 GHz.

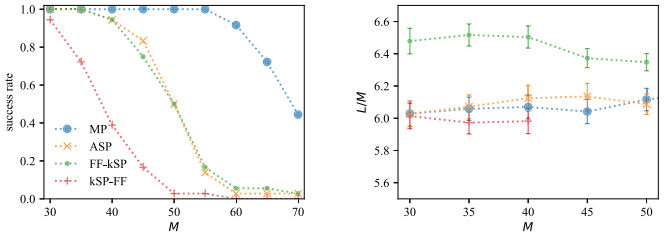

(a) success rate (b) average path length

FIG. 15. Numerical solutions on network CONUS60 under the EDP constraint for $Q = 10$ by our algorithm (MP) and three commonly used heuristics: k-shortest-path first fit (kSP-FF, $k = 10$ in the experiments), first fit k-shortest-path (FF-kSP) and adaptive shortest-path routing (ASP). (a) Presents the success rate, the fraction of communicated requests for which a valid route can be found. (b) Average path length, for the communicated requests with valid routes only. The results were obtained by averaging over 36 randomly samples communication requests per point.

fraction of a second, variable signal to noise ratio per edge and many more. All of these can be accommodated within our framework; some of these extensions are detailed below.

In real optical networks, the number of wavelength channels in different optical fibers may vary; their lengths, signal-to-noise ratios, or type of fibers used may influence the quality of communication. To make our model more general and realistic, we consider the case of optical networks with weight $w_{i,j}$ and number of wavelengths $Q_{i,j}$ defined for any individual link (i, j) (or Q_i defined for node i in node-disjoint wavelength-switching scenarios). With simple modifications, our proposed algorithm can be generalized to accommodate $w_{i,j}$, $Q_{i,j}$, or Q_i.

In cases with heterogeneous $Q_{i,j}$ on edges, we denote the largest number of wavelength channels among all edges to be Q_*, i.e., $Q_* = \max_{(i,j)} Q_{i,j}$, then for an edge (i, j), one can introduce $Q_* - Q_{i,j}$ additional wavelength channels with state 0, such that all edges on the network would have virtually Q_* wavelengths.

As for heterogeneous weights on edges with linear cost, the objective function becomes $L = \sum_{(i,j)} w_{i,j} \sum_{a=1}^{Q} (1 - \delta^0_{s^a_{i,j}})$ and the partition function in Eq. (2) becomes

$$Z(\beta) = \sum_{\vec{s}} \Omega(\vec{s}) \prod_{(i,j)} e^{-\beta w_{i,j} F_{i,j}(\vec{s}_{i,j})}. \tag{32}$$

A. Heterogeneous wavelength availability on edges

In the message-passing Eqs. (13) describing NDP scenario, the first equation $\phi^a_{i\to j}(0)$ considers the condition for wavelength a of edge (i, j) to be in state 0 in the absence of node j, and the contribution to the objective function L is 0; this equation is the same in cases with heterogeneous edge weights. Nevertheless, weights $w_{i,j}$ should be introduced in the second equation as

$$\phi^a_{i\to j}(s) = w_{i,j} + \min_{k\in\partial i\setminus j} \left[\phi^a_{k\to i}(s) + \sum_{l\in\partial i\setminus j,k} \phi^a_{l\to i}(0) \right]. \tag{33}$$

The same applies for the EDP scenarios and the second message-passing equation in Eq. (23) should be modified as follows:

$$\phi^a_{i\to j}(s) = w_{i,j} + \min_{k\in\partial i\setminus j} \left[\phi^a_{k\to i}(s) + \min_{\substack{\text{matched} \\ \text{pairs:}\vec{s}_{\partial i\setminus j,k}}} \sum_{l\in\partial i\setminus j,k} \phi^a_{l\to i}(s_l) \right]. \tag{34}$$

The marginal messages on edges, Eq. (14), should be modified as

$$\phi^a_{i,j}(s) = \phi^a_{i\to j}(s) + \phi^a_{j\to i}(-s) + w_{i,j}\left(\delta^0_s - 1\right). \tag{35}$$

The same algorithmic procedure described in Sec. III C can be applied in the present cases with heterogeneous edge weights.

For an even more general scenarios, our model can be modified to accommodate heterogeneous weights for different wavelength channels on the same edge, i.e., $w^a_{i,j} \neq w^b_{i,j}$ for $a \neq b$, asymmetric directed weights such as $w_{i,j} \neq w_{j,i}$ on directed graphs. In these cases, one only needs to replace $w_{i,j}$ in the above modified equations by $w^a_{i,j}$ or directed weights.

B. Heterogeneous wavelength availability on nodes with wavelength-switching

For the NDP scenarios with heterogeneous wavelength availability on nodes, we do not have to introduce additional wavelengths and keep unavailable channels in state 0 if Q_i are nonuniform; this is because the equation of node capacity constraint Eq. (16) has already considered the case of different Q_i values. Only the second equation of Eq. (15) needs to be modified, which reads

$$\phi^{\mu}_{i\to j}(\pm 1) = w_{i,j} + \tau^{\mu}_{i}(1) + \min_{k\in\partial i\setminus j}\left[\phi^{\mu}_{k\to i}(\pm 1) + \sum_{l\in\partial i\setminus j,k}\phi^{\mu}_{l\to i}(0)\right]. \quad (36)$$

VI. CONCLUSION

Multiwavelength NDP/EDP routing lies at the heart of the efficient running and design of optical communication networks, that act as the backbone of the internet. One of the key questions in running optical communication networks more efficiently is in the ability to carry out these routing tasks effectively for large systems. This serves for both day-to-day running of the network as well as for the design of new networks and the modification of existing infrastructure. While principled *single wavelength* NDP and EDP routing algorithms based on message passing have been developed already, they could not be employed in real optical networks due to the difficulty in extending the algorithms from the single wavelength to the multiwavelength case. A straightforward extension of existing single-wavelength EDP/NDP routing algorithms would result in a prohibitive computational cost that grows exponentially with the system size.

To accommodate a large number of wavelengths and transmissions in large systems, we have developed algorithmic solutions that include multilayer graphs, where each layer represents a different wavelength, and messages are passed within layer (routing assignment) and between layers (wavelength allocation). The scalable algorithm we have devised shows very good performance in manageable timescales.

We expect the algorithm to be implemented in realistic scenarios, where specific aspects of real network routing, such as heterogeneous wavelength availability and signal-to-noise ratios will have to be added in the manner outlined in Sec. V. While these extensions and many others can be straightforwardly accommodated within our framework, they should be carefully integrated and tested to comply with existing routing methods, traffic conditions and existing protocols. This would require dedicated work on specific applications. We also expect the algorithm to be utilized for network design and see several possible extensions for both localized and global message passing-based implementation. Utilization of the algorithms developed here in ad-hoc network communication, multilayer VLSI design and multilayer networks will require further study of the specific requirements for the different applications.

ACKNOWLEDGMENTS

D.S. and Y.Z.X. acknowledge support from the Engineering and Physical Sciences Research Council (EPSRC) Programme Grant TRANSNET (Grant No. EP/R035342/1) and thank Caterina De Bacco for pointing us to her code available on GitHub. The work by C.H.Y. and H.F.P. is supported by the Research Grants Council of the Hong Kong Special Administrative Region, China (Projects No. EdUHK GRF 18304316, No. GRF 18301217, and No. GRF 18301119), the Dean's Research Fund of the Faculty of Liberal Arts and Social Sciences (Projects No. FLASS/DRF 04418, No. FLASS/ROP 04396, and No. FLASS/DRF 04624), and the Internal Research Grant (Project No. RG67 2018-2019R R4015 and No. RG31 2020-2021R R4152), The Education University of Hong Kong, Hong Kong Special Administrative Region, China. D.S. and Y.Z.X. thank Ruijie Luo, Robin Matzner, and Polina Bayvel for insightful comments on practical routing in optical communication systems.

APPENDIX: FACTOR GRAPH

Due to the interaction between wavelength allocation per request (layers) and the routing in the physical network per layer, the resulting factor graphs are loopy, even when the original graph is a tree. Message passing techniques have been shown to provide good solutions in loopy graphs below a critical ratio between constraints and free variables [41], so that it is not surprising that they are successful also in this case. Additionally, routing in optical communication networks operates well below this critical ratio, for obvious reasons, and it is also unclear what this critical ratio is for routing problems in general and multiwavelength NDP, EDP and WS routing in particular. Nevertheless, to clarify the factor graph in the various scenarios we provide Figs. 16 and 17.

A natural question is the reason behind the demonstrated success of the algorithm given the loopy structure of the factor graphs. In the case of linear cost with either NDP or EDP

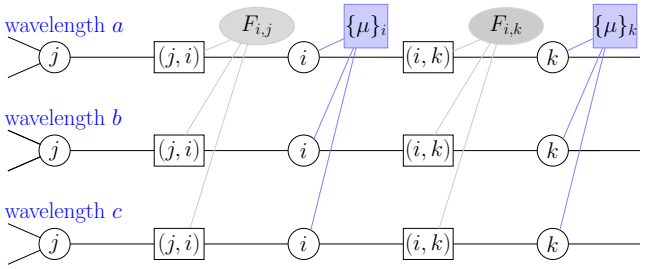

FIG. 16. Factor graph for the NDP/EDP routing model, where the state of nodes, edges in the original graph and cost function are represented by circles (i, j …), rectangles (variable pairs (i, j)) and ellipse factors ($F_{i,k}$), respectively. The allocation of request pairs to nodes in wavelength layers and the interaction between them are represented by the light-purple square factor ($\{\mu\}_i$). The cost of an edge $F_{i,k}$ depends on the state of the edge (i,k) for all wavelengths; the state of an edge (i,k) for a given wavelength is restricted by the state of the neighboring nodes i and k using the same wavelength per request and the cross-wavelength cost $F_{i,k}$. If the cost function $F_{i,k}$ is linear, then the model can be simplified and the ellipse factors can be omitted.

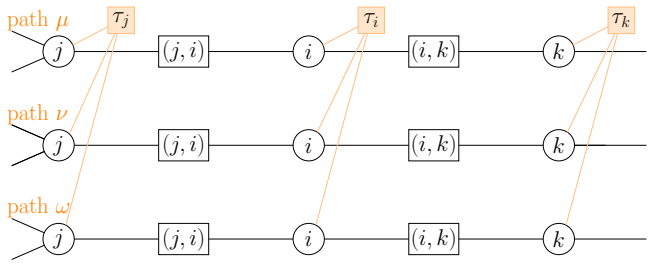

FIG. 17. Factor graph for the WS routing model, where the state of nodes, edges and cost functions are represented by circle (i), rectangle ($i, j \ldots$) and wavelength-constraint square (τ_i) factors, respectively. The latter merely validates that the number of lightpaths going through a node does not exceed the total number of lightpaths.

constraints, different wavelength layers interact only through the origins and destinations ($\{\mu\}_i$), and if the original graph is acyclic, then we expect only loops of larger size to exist.

In cases with nonlinear costs on edges, interactions between layers are found on every edge ($F_{i,k}$), and hence the resulting graphs are loopy for both NDP and EDP scenarios. Nevertheless, the loopy cross-wavelength interaction is relatively weak with respect to the interaction along the entire lightpath and the contiguity constraint. More specifically, in the EDP/NDP cases the cross-layer interaction is independent of the specific wavelength assignment as it only depends on the *number* of wavelengths used per edge, while messages within layers are a results of a complete trajectory of interaction between nodes and edges, verifying contiguity, wavelength availability and edge load.

For the WS scenario, since interlayer links are present at every node, we expect that the factor graph to be very loopy. However, cross-layer interactions in the WS scenario are extremely weak the only requirement enforced by the factor τ_i for node i is that there are enough available wavelengths to accommodate the number of lightpaths; in a way, WS can be viewed as an extended version of single wavelength NDP where a number of lightpaths through a node is being limited to Q. We believe these are the reasons for the demonstrated success of the method, even for small loopy graphs as demonstrated in Table II.

[1] A. D. Ellis, N. M. Suibhne, D. Saad, and D. N. Payne, Communication networks beyond the capacity crunch, Philos. Trans. R. Soc. A. **374**, 20150191 (2016).

[2] H. Zang, J. P. Jue, and B. Mukherjee, A review of routing and wavelength assignment approaches for wavelength-routed optical WDM networks, Opt. Netw. Mag. **1**, 47 (2000).

[3] B. C. Chatterjee, N. Sarma, and P. P. Sahu, Review and performance analysis on routing and wavelength assignment approaches for optical networks, IETE Tech. Rev. **30**, 12 (2013).

[4] M. Biswanath, T. Ioannis, T. Massimo, W. Peter, and Z. Yongli, *Springer Handbook of Optical Networks* (Springer, Berlin, 2020).

[5] B. Corcoran, M. Tan, X. Xu, A. Boes, J. Wu, T. Nguyen, S. Chu, B. Little, R. Morandotti, A. Mitchell, and D. Moss, Ultra-dense optical data transmission over standard fibre with a single chip source, Nat. Commun. **11**, 2568 (2020).

[6] C. H. Yeung and D. Saad, Competition for Shortest Paths on sparse graphs, Phys. Rev. Lett. **108**, 208701 (2012).

[7] C. H. Yeung, D. Saad, and K. M. Wong, From the physics of interacting polymers to optimizing routes on the london underground, Proc. Natl. Acad. Sci. USA **110**, 13717 (2013).

[8] C. H. Yeung, Coordinating dynamical routes with statistical physics on space-time networks, Phys. Rev. E **99**, 042123 (2019).

[9] H. F. Po, C. H. Yeung, and D. Saad, Futility of being selfish in optimized traffic, Phys. Rev. E **103**, 022306 (2021).

[10] C. De Bacco, S. Franz, D. Saad, and C. H. Yeung, Shortest node-disjoint paths on random graphs, J. Stat. Mech.: Theory Exp. (2014) P07009.

[11] F. Altarelli, A. Braunstein, L. DallAsta, C. De Bacco, and S. Franz, The edge-disjoint path problem on random graphs by message-passing, PLoS One **10**, e0145222 (2015).

[12] R. Karp, Reducibility among combinatorial problems, in *Complexity of Computer Computations* (Springer, Berlin, 1972), pp. 85–103.

[13] M. R. Garey and D. S. Johnson, *Computers and Intractability: A Guide to the Theory of NP-Completeness (Series of Books in the Mathematical Sciences)*, 1st ed. (W. H. Freeman, New York, NY, 1979).

[14] B. Korte and J. Vygen, Multicommodity flows and edge-disjoint paths, in *Combinatorial Optimization: Theory and Algorithms* (Springer, Berlin, 2012), pp. 489–520.

[15] T. Erlebach, Approximation algorithms for edge-disjoint paths and unsplittable flow, in *Efficient Approximation and Online Algorithms: Recent Progress on Classical Combinatorial Optimization Problems and New Applications*, edited by E. Bampis, K. Jansen, and C. Kenyon (Springer, Berlin, 2006), pp. 97–134.

[16] N. Robertson and P. Seymour, Graph minors. XIII: The disjoint paths problem, J. Comb. Theory, Ser. B **63**, 65 (1995).

[17] J. Vygen, Disjoint paths, Tech. Rep. Report No 94816 (Research Institute of Discrete Mathematics, University of Bonn, 1994).

[18] J. Vygen, Np-completeness of some edge-disjoint paths problems, Discrete Appl. Math. **61**, 83 (1995).

[19] D. Banerjee and B. Mukherjee, A practical approach for routing and wavelength assignment in large wavelength-routed optical networks, IEEE J. Sel. Areas Commun. **14**, 903 (1996).

[20] S. G. Kolliopoulos and C. Stein, *Approximating disjoint-path problems using packing integer programs* (Springer-Verlag, Berlin, 1998), pp. 153–168.

[21] A. E. Ozdaglar and D. P. Bertsekas, Routing and wavelength assignment in optical networks, IEEE/ACM Trans. Netw. **11**, 259 (2003).

[22] A. Baveja and A. Srinivasan, Approximation algorithms for disjoint paths and related routing and packing problems, Math. Oper. Res. **25**, 2000 (2000).

[23] M. Klinkowski, M. Otkiewicz, K. Walkowiak, M. Piro, M. Ruiz, and L. Velasco, Solving large instances of the RSA problem in flexgrid elastic optical networks, IEEE/OSA J. Opt. Commun. Netw. **8**, 320 (2016).

[24] N. Skorin-Kapov, Routing and wavelength assignment in optical networks using bin packing based algorithms, Eur. J. Op. Res. **177**, 1167 (2007).

[25] Q. D. Pham, Y. Deville, and P. Hentenryck, Ls(graph): A constraint-based local search for constraint optimization on trees and paths, Constraints **17**, 357 (2012).

[26] L. Belgacem, I. Charon, and O. Hudry, A post-optimization method for the routing and wavelength assignment problem applied to scheduled lightpath demands, Eur. J. Oper. Res. **232**, 298 (2014).

[27] C. Chen and B. Banerjee, A new model for optimal routing and wavelength assignment in wavelength division multiplexed optical networks, in *Proceedings of the 15th Annual Joint Conference of the IEEE Computer Societies. Networking the Next Generation (INFOCOM'96)*, Vol. 1 (IEEE, 1996), pp. 164–171.

[28] Z. Sumpter, L. Burson, B. Tang, and X. Chen, Maximizing number of satisfiable routing requests in static ad hoc networks, in *2013 IEEE Global Communications Conference (GLOBECOM)* (IEEE, Piscataway, NJ, 2013), pp. 19–24.

[29] A. Srinivas and E. Modiano, Minimum energy disjoint path routing in wireless ad-hoc networks, in *Proceedings of the 9th Annual International Conference on Mobile Computing and Networking* (ACM, New York, NY, 2003), pp. 122–133.

[30] P. Manohar, D. Manjunath, and R. K. Shevgaonkar, Routing and wavelength assignment in optical networks from edge disjoint path algorithms, IEEE Commun. Lett. **6**, 211 (2002).

[31] T. F. Noronha, M. G. C. Resende, and C. C. Ribeiro, A biased random-key genetic algorithm for routing and wavelength assignment, J. Glob. Optim. **50**, 503 (2010).

[32] R. Storn and K. V. Price, Differential evolution—A simple and efficient heuristic for global optimization over continuous spaces, J. Glob. Optim. **11**, 341 (1997).

[33] C. Hsu and H.-J. Cho, A genetic algorithm for the maximum edge-disjoint paths problem, Neurocomputing **148**, 17 (2015).

[34] M. Blesa and C. Blum, Ant colony optimization for the maximum edge-disjoint paths problem, in *Proceedings of the Workshops on Applications of Evolutionary Computation* (Springer, Berlin, 2004), pp. 160–169.

[35] C.-C. Hsu, H.-J. Cho, and S.-C. Fang, Solving routing and wavelength assignment problem with maximum edge-disjoint paths, J. Ind. Manage. Optim. **13**, 1065 (2017).

[36] E. Agrell, M. Karlsson, A. R. Chraplyvy, D. J. Richardson, P. M. Krummrich, P. Winzer, K. Roberts, J. K. Fischer, S. J. Savory, B. J. Eggleton, M. Secondini, F. R. Kschischang, A. Lord, J. Prat, I. Tomkos, J. E. Bowers, S. Srinivasan, M. Brandt-Pearce, and N. Gisin, Roadmap of optical communications, J. Opt. **18**, 063002 (2016).

[37] P. Bayvel, R. Maher, T. Xu, G. Liga, N. A. Shevchenko, D. Lavery, A. Alvarado, and R. I. Killey, Maximizing the optical network capacity, Philos. Trans. R. Soc. A **374**, 20140440 (2016).

[38] M. Mézard, G. Parisi, and M. A.Virasoro, *Spin Glass Theory and Beyond* (World Scientific, Singapore, 1987), Vol. 9.

[39] J. Pearl, Reverend Bayes on inference engines: A distributed hierarchical approach, in *Proceedings of the 2nd National Conference on Artificial Intelligence (AAAI'82)* (AAAI Press, Palo Alto, CA, 1982), pp. 133–136.

[40] R. Gallager, Low-density parity-check codes, IRE Trans. Inf. Theory **8**, 21 (1962).

[41] M. Mézard and A. Montanari, *Information, Physics, and Computation* (Oxford University Press, Oxford, UK, 2009).

[42] Y. Kabashima and D. Saad, Belief propagation vs. TAP for decoding corrupted messages, Europhys. Lett. **44**, 668 (1998).

[43] P. Erdös and A. Rényi, On random graphs I, Publ. Math. Debrecen **6**, 290 (1959).

[44] J.-P. Onnela, J. Saramki, J. Hyvnen, G. Szab, D. Lazer, K. Kaski, J. Kertsz, and A.-L. Barabsi, Structure and tie strengths in mobile communication networks, Proc. Natl. Acad. Sci. USA **104**, 7332 (2007).

[45] P. Wright, A. Lord, and S. Nicholas, Comparison of optical spectrum utilization between flexgrid and fixed grid on a real network topology, in *Proceedings of the Optical Fiber Communication Conference* (Optica Publishing Group, Washington, DC, 2012).

[46] Monarch Network Architects, 60-node network derived from the coronet conus topology, retrieved from http://monarchna.com/60-Node-CONUS-Topology.xls.

[47] K. Sato, H. Hasegawa, T. Niwa, and T. Watanabe, A large-scale wavelength routing optical switch for data center networks, IEEE Commun. Mag. **51**, 46 (2013).

[48] O. Gerstel, M. Jinno, A. Lord, and S. J. B. Yoo, Elastic optical networking: A new dawn for the optical layer? IEEE Commun. Mag. **50**, s12 (2012).

[49] B. Teipen, M. Eiselt, K. Grobe, and J.-P. Elbers, Adaptive data rates for flexible transceivers in optical networks, J. Netw. **7**, 776 (2012).

[50] K. Akkaya and M. Younis, A survey on routing protocols for wireless sensor networks, Ad Hoc Netw. **3**, 325 (2005).

[51] A. Aggarwal, J. Kleinberg, and D. P.Williamson, Node-disjoint paths on the mesh and a new trade-off in VLSI layout, in *Proceedings of the 28th Annual ACM Symposium on Theory of Computing* (ACM, New York, NY, 1996), pp. 585–594.

[52] C. Chekuri and A. Ene, Poly-logarithmic approximation for maximum node disjoint paths with constant congestion, in *Proceedings of the Symposium on Discrete Algorithms (SODA'13)* (ACM, New York, NY, 2013), pp. 326–341.

[53] M. M and P. G, The cavity method at zero temperature, J. Stat. Phys. **111**, 1 (2003).

[54] H. Bethe, Statistical theory of superlattices, Proc. R. Soc. London A **150**, 552 (1935).

[55] M. Mézard and G. Parisi, The Bethe lattice spin glass revisited, Eur. Phys. J. B **20**, 217 (2001).

[56] M.-A. Badiu, D. Saad, and J. P. Coon, Self-organization scheme for balanced routing in large-scale multihop networks, J. Phys. A: Math. Theor. **54**, 045001 (2021).

[57] L. Lovász and M. D. Plummer, *Matching Theory* (American Mathematical Society, Providence, RI, 2009), Vol. 367.

[58] Z. Galil, S. Micali, and H. Gabow, An $o(ev \log v)$ algorithm for finding a maximal weighted matching in general graphs, SIAM J. Comput. **15**, 120 (1986).

[59] G. Yan, T. Zhou, B. Hu, Z. Q. Fu, and B. H. Wang, Efficient routing on complex networks, Phys. Rev. E: Stat., Nonlinear, Soft Matter Phys. **73**, 046108 (2006).

[60] D. J. Ives, P. Bayvel, and S. J. Savory, Routing, modulation, spectrum, and launch power assignment to maximize the traffic throughput of a nonlinear optical mesh network, Photon. Netw. Commun. **29**, 244 (2015).

[61] K. Potou, K. Manousakis, K. Christodoulopoulos, and E. Varvarigos, Dynamic routing and wavelength assignment in transparent WDM networks with amplifiers' power constraints, in *Proceedings of the Future Network and Mobile Summit* (IEEE, Piscataway, NJ, 2010), p. 1557.

[62] Y. Wang, T. H. Cheng, and M. H. Lim, A tabu search algorithm for static routing and wavelength assignment problem, IEEE Commun. Lett. **9**, 841 (2005).

[63] R. S. Barpanda, A. K. Turuk, B. Sahoo, and B. Majhi, Genetic algorithm approaches to solve rwa problem in wdm optical networks, in *Proceedings of the International Conference on Swarm, Evolutionary, and Memetic Computing* (Springer, Berlin, 2010), pp. 599–606.

[64] I. Martin, J. A. Hernandez, S. Troia, F. Musumeci, G. Maier, and O. G. de Dios, *Is machine learning suitable for solving RWA problems in optical networks?* In *Proceedings of the European Conference on Optical Communication (ECOC'18)* (IEEE, Piscataway, NJ, 2018), pp. 1–3.

[65] I. Martin, S. Troia, J. A. Hernandez, A. Rodriguez, F. Musumeci, G. Maier, R. Alvizu, and O. G. de Dios, Machine learning-based routing and wavelength assignment in software-defined optical networks, IEEE Trans. Netw. Serv. Manage. **16**, 871 (2019).

[66] R. Ramaswami and K. Sivarajan, Design of logical topologies for wavelength-routed optical networks, IEEE J. Sel. Areas Commun. **14**, 840 (1996).

[67] S. Jain, A. Kumar, S. Mandal, J. Ong, L. Poutievski, A. Singh, S. Venkata, J. Wanderer, J. Zhou, M. Zhu *et al.*, B4: Experience with a globally-deployed software defined WAN, ACM SIGCOMM Comput. Commun. Rev. **43**, 3 (2013).

[68] D. Monoyios and K. Vlachos, Multiobjective genetic algorithms for solving the impairment-aware routing and wavelength assignment problem, J. Opt. Commun. Netw. **3**, 40 (2011).

[69] R. J. Vincent, D. J. Ives, and S. J. Savory, Scalable capacity estimation for nonlinear elastic all-optical core networks, J. Lightwave Technol. **37**, 5380 (2019).